

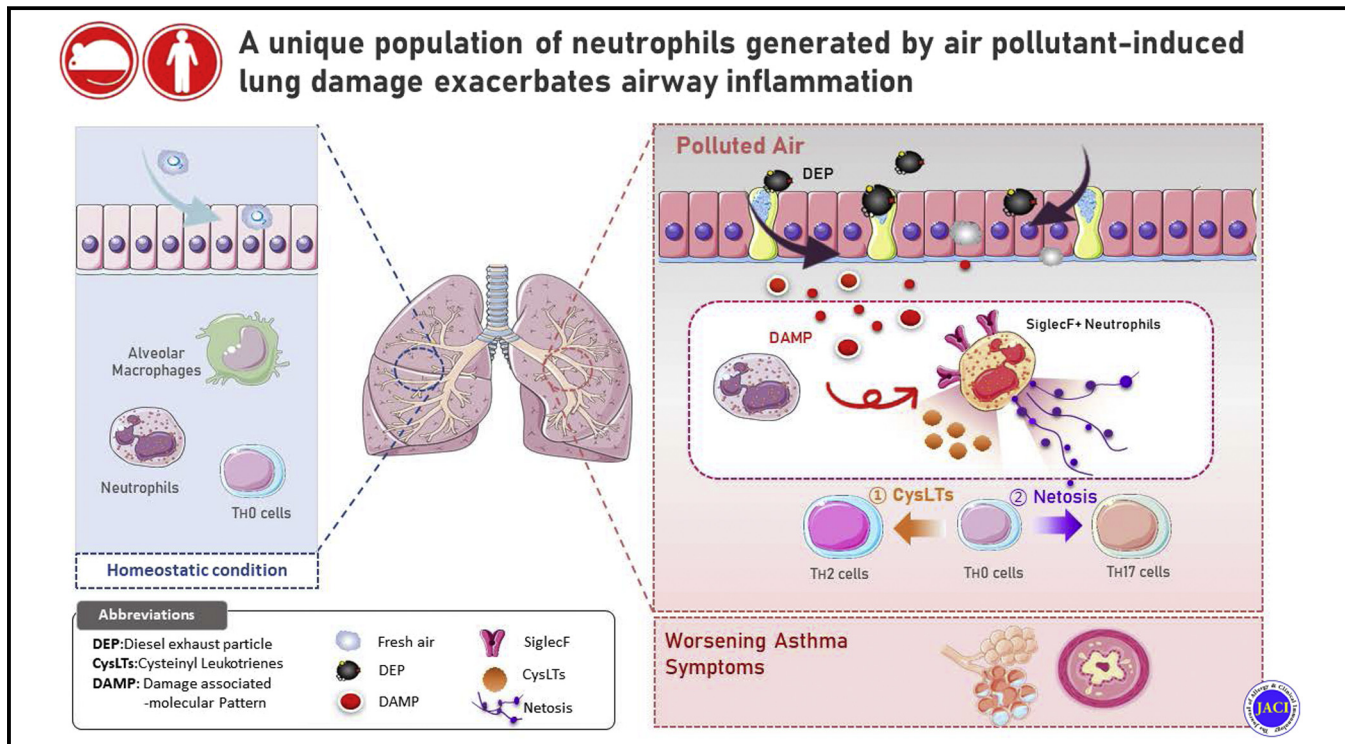
# A unique population of neutrophils generated by air pollutant-induced lung damage exacerbates airway inflammation

 Check for updates

Jae Woo Shin, BS,<sup>a</sup> Jihyun Kim, PhD,<sup>a</sup> Seokjin Ham, PhD,<sup>b</sup> Sun Mi Choi, MD, MS,<sup>c</sup> Chang-Hoon Lee, MD, PhD,<sup>c</sup> Jung Chan Lee, PhD,<sup>d</sup> Ji Hyung Kim, PhD,<sup>e</sup> Sang-Heon Cho, MD, PhD,<sup>f,g</sup> Hye Ryun Kang, MD, PhD,<sup>f,g</sup> You-Me Kim, PhD,<sup>h</sup> Doo Hyun Chung, MD, PhD,<sup>i,j</sup> Yeonseok Chung, PhD,<sup>k</sup> Yoe-Sik Bae, PhD,<sup>l,m</sup> Yong-Soo Bae, PhD,<sup>l,m</sup> Tae-Young Roh, PhD,<sup>b,n</sup> Taesoo Kim, PhD,<sup>o</sup> and Hye Young Kim, PhD<sup>a,g</sup>

Seoul, Pohang, Daejeon, and Suwon, Korea

### GRAPHICAL ABSTRACT



From <sup>a</sup>the Laboratory of Mucosal Immunology in Department of Biomedical Sciences, Seoul National University College of Medicine, Seoul, <sup>b</sup>the Department of Life Sciences and Division of Integrative Biosciences & Biotechnology, Pohang University of Science & Technology (POSTECH), Pohang, <sup>c</sup>the Department of Internal Medicine, Seoul National University Hospital, Seoul, <sup>d</sup>the Department of Biomedical Engineering, Seoul National University College of Medicine, Seoul, <sup>e</sup>the College of Life Sciences and Biotechnology, Korea University, Seoul, <sup>f</sup>the Division of Allergy and Clinical Immunology, Department of Internal Medicine, Seoul National University College of Medicine, Seoul, <sup>g</sup>the Institute of Allergy and Clinical Immunology, Seoul National University Medical Research Center, Seoul National University College of Medicine, Seoul, <sup>h</sup>the Graduate School of Medical Science and Engineering, Korea Advanced Institute of Science and Technology, Daejeon, <sup>i</sup>the Department of Pathology, Seoul National University College of Medicine, Seoul, <sup>j</sup>the Laboratory of Immune Regulation in Department of Biomedical Sciences, Seoul National University College of Medicine, Seoul, <sup>k</sup>the Laboratory of Immune Regulation, Research Institute of Pharmaceutical Sciences, College of Pharmacy, Seoul National University, Seoul, <sup>l</sup>the Department of Biological Sciences, SRC Center for Immune Research on Non-lymphoid Organs, Sungkyunkwan University, Suwon, <sup>m</sup>the Department of Biological Sciences, Sungkyunkwan University, Suwon, <sup>n</sup>SysGenLab Inc, Pohang, and <sup>o</sup>the Department of Life Science, Ewha Womans University, Seoul.

This study was supported by grants from the Korea Healthcare Technology R&D Project of the Ministry of Health and Welfare, Korea (HI15C1736) and a grant from the National Research Foundation of Korea (NRF-2019R1A2C2087574 and SRC 2017R1A5A1014560). Jae Woo Shin received a scholarship from the BK21-plus education program provided by the National Research Foundation of Korea.

Disclosure of potential conflict of interest: The authors declare that they have no relevant conflicts of interest.

Received for publication February 23, 2021; revised August 26, 2021; accepted for publication September 2, 2021.

Available online October 20, 2021.

Corresponding author: Hye Young Kim, PhD, Laboratory of Mucosal Immunology, Department of Biomedical Sciences, Seoul National University College of Medicine 103 Daehak-ro, Jongno-gu, Seoul 03080, Republic of Korea. E-mail: [hykim11@snu.ac.kr](mailto:hykim11@snu.ac.kr)

 The CrossMark symbol notifies online readers when updates have been made to the article such as errata or minor corrections

0091-6749/\$36.00

© 2021 American Academy of Allergy, Asthma & Immunology  
<https://doi.org/10.1016/j.jaci.2021.09.031>

**Background:** Diesel exhaust particles (DEPs) are the main component of traffic-related air pollution and have been implicated in the pathogenesis and exacerbation of asthma. However, the mechanism by which DEP exposure aggravates asthma symptoms remains unclear.

**Objective:** This study aimed to identify a key cellular player of air pollutant-induced asthma exacerbation and development.

**Methods:** We examined the distribution of innate immune cells in the murine models of asthma induced by house dust mite and DEP. Changes in immune cell profiles caused by DEP exposure were confirmed by flow cytometry and RNA-Seq analysis. The roles of sialic acid-binding, Ig-like lectin F (SiglecF)-positive neutrophils were further evaluated by adoptive transfer experiment and *in vitro* functional studies.

**Results:** DEP exposure induced a unique population of lung granulocytes that coexpressed Ly6G and SiglecF. These cells differed phenotypically, morphologically, functionally, and transcriptionally from other SiglecF-expressing cells in the lungs. Our findings with murine models suggest that intratracheal challenge with DEPs induces the local release of adenosine triphosphate, which is a damage-associated molecular pattern signal. Adenosine triphosphate promotes the expression of SiglecF on neutrophils, and these SiglecF<sup>+</sup> neutrophils worsen type 2 and 3 airway inflammation by producing high levels of cysteinyl leukotrienes and neutrophil extracellular traps. We also found Siglec8- (which corresponds to murine SiglecF) expressing neutrophils, and we found it in patients with asthma–chronic obstructive pulmonary disease overlap.

**Conclusion:** The SiglecF<sup>+</sup> neutrophil is a novel and critical player in airway inflammation and targeting this population could reverse or ameliorate asthma. (*J Allergy Clin Immunol* 2022;149:1253–69.)

**Key words:** Diesel exhaust particles, granulocytes, SiglecF, ATP, DAMP, neutrophil extracellular traps, leukotrienes, asthma

Not only is asthma the most common chronic airway disease in the world, but also its prevalence continues to rise in many parts of the world.<sup>1</sup> Asthma is characterized by the clinical syndromes of bronchial hyperresponsiveness, inflammation, and reversible airflow obstruction.<sup>2,3</sup> Epidemiologic studies have identified several environmental risk factors that may largely account for the increasing prevalence of asthma. These include air pollutants such as cigarette smoke, mold, sulfur dioxide, nitrogen oxide, ozone, and inhalable particulate matter; all are known to trigger asthma in susceptible individuals.<sup>4</sup> Of particular interest to this study are diesel exhaust particulates (DEPs), which have been strongly implicated in both the development and the exacerbation of asthma.<sup>5</sup> DEPs comprise the main components of inhalable particulate matter, and respiratory exposure to DEPs leads to marked oxidative stress and epithelial damage and then production of numerous proinflammatory cytokines and chemokines in the lungs.<sup>6,7</sup> Given the large burden of asthmatic disease and the importance of the lungs as frontline organs that react to airborne allergens, it is critical to understand the respiratory immune responses to air pollutants such as DEPs.

Asthma is not a single disease; rather, the term encompasses a variety of phenotypes. These phenotypes remain vague at present,

#### Abbreviations used

ACO:	Asthma–chronic obstructive pulmonary disease overlap
AHR:	Airway hyperresponsiveness
ATP:	Adenosine triphosphate
BAL:	Bronchoalveolar lavage
BM:	Bone marrow
CitH3:	Citrullinated histone H3
CysLT:	Cysteinyl leukotriene
DAMP:	Damage-associated molecular pattern
DEP:	Diesel exhaust particulate
DMSO:	Dimethyl sulfoxide
dsDNA:	Double-stranded DNA
FACS:	Fluorescence-activated cell sorting
GO:	Gene Ontology ( <a href="http://geneontology.org/">http://geneontology.org/</a> )
HDM:	House dust mite
IF:	Immunofluorescence
ILC:	Innate lymphoid cell
LPS:	Lipopolysaccharide
LTC <sub>4</sub> :	Leukotriene C <sub>4</sub>
Ltc4s:	Leukotriene C <sub>4</sub> synthase
MPO:	Myeloperoxidase
NET:	Neutrophil extracellular trap
OVA:	Ovalbumin
PBS:	Phosphate-buffered saline
PBS-T:	PBS containing 0.05% Tween 20
PGD <sub>2</sub> :	Prostaglandin D <sub>2</sub>
ROS:	Reactive oxidative species
SiglecF:	Sialic acid-binding, Ig-like lectin F

but the best known is allergic asthma, which, broadly speaking, presents with an early onset, corticosteroid responsiveness, excessive type 2 immune responses, eosinophilia, and allergen-specific IgE that drive airway hyperresponsiveness (AHR), which is the cardinal feature of asthma.<sup>8,9</sup> The cells that participate in the pathophysiology of allergic asthma include dendritic cells, which recognize asthmogenic allergens, pollutants, and viruses and initiate powerful adaptive type 2 immune responses.<sup>10</sup> These responses in turn activate eosinophils, which contribute to airway remodeling in allergic asthma.<sup>11,12</sup> Mast cells also play an important role in allergic asthma by controlling the early- and late-phase allergic responses and contributing to smooth muscle contraction.<sup>13</sup>

The strong focus in the field on allergic asthma means that relatively little is known about the other immune cells that participate in asthma pathogenesis. This includes neutrophils, which, like eosinophils, are granulocytes. There has been speculation that neutrophilic asthma is phenotypically different from eosinophilic asthma.<sup>14,15</sup> McKinley et al<sup>16</sup> showed that neutrophils are associated with exacerbations of poorly controlled and steroid-resistant asthma. Goleva et al<sup>17</sup> found that steroid-resistant asthma is associated with higher levels of neutrophil-recruiting chemokines in bronchoalveolar lavage (BAL) fluid. In addition, neutrophilic asthma is thought to be driven by type 3 immunity (namely IL-17A from T<sub>H</sub>17 and type 3 innate lymphoid cells [ILC3s]),<sup>18,19</sup> whereas eosinophilic asthma phenotypes are thought to be mainly driven by type 2 immunity. However, multiple lines of evidence also suggest that neutrophils contribute to allergic asthma as well; for example, impairing neutrophil recruitment decreases the classical type 2 immune responses that drive allergic asthma.<sup>20</sup> Interestingly, Toussaint

et al<sup>21</sup> showed in 2017 that allergic asthma exacerbations associate with the rhinovirus-induced release of neutrophil extracellular traps (NETs). NETs contain citrullinated histone H3 (CitH3), granule proteins, and decondensed chromatin and permit neutrophils to kill extracellular pathogens while limiting host cell damage.<sup>22</sup> Similarly, the study of Goleva et al<sup>17</sup> found that patients with steroid-resistant neutrophilic-type asthma had higher levels of environmental endotoxin in their BAL fluid than patients with corticosteroid-sensitive asthma. These observations together suggest first that environmental factors such as viruses and endotoxin can promote asthma, and second that neutrophils may mediate this phenomenon.

Because DEPs also induce asthma exacerbations,<sup>5</sup> we were interested in elucidating the cellular and molecular mechanisms by which this environmental pollutant affects the development of asthma. In the present study, we identified a distinct population of neutrophils that coexpresses the neutrophil marker Ly6G and the immunoreceptor sialic acid–binding, Ig-like lectin F (SiglecF) in a preclinical model of air pollutant (DEP)-induced asthma that incorporates both type 2 and type 3 immune responses. We also detected similar neutrophils in the peripheral blood and sputum of patients with asthma–chronic obstructive pulmonary disease overlap (ACO). Our observations together showed that air pollutants could generate a novel neutrophil population that is characterized by high NET and cysteinyl leukotriene (CysLT) release, which elevate both type 2 and type 3 immune responses and thereby augment AHR.

## METHODS

### Mice

Female C57BL/6 mice, aged 7 to 8 weeks, were purchased from Koatech (Pyeongtaek, Republic of Korea). ΔdblGATA mice, aged 7 to 8 weeks, were kindly provided by Professor You-Me Kim (Postech, Pohang, Republic of Korea). All experiments described here were approved by the Institutional Animal Care and Use Committee of Seoul National University Hospital (SNUH-IACUC 18-0269-S1A1). Animals were maintained in an Association for the Assessment and Accreditation of Laboratory Animal Care internationally accredited facility (#001169) and were cared for according to the 8th edition (2010) of the Guide for the Care and Use of Laboratory Animals of the National Resource Council.

### Murine models of air pollutant or adenosine triphosphate-induced lung inflammation and asthma

To mimic air pollutant exposure, 150 µg of DEP (Standard Reference Material 1650b; National Institute for Standards and Technology, Gaithersburg, Md) was dissolved in 6% dimethyl sulfoxide (DMSO) and sonicated at approximately 20% to 25% of amplitude for 10 minutes. DEP was instilled into isoflurane-anesthetized mice intratracheally. To induce asthma, 10 µg of house dust mites (HDMs; *Der p*; Greer, Lenoir, NC) were suspended and intratracheally instilled on days 0, 7, 8, and 9. For HDM asthma exacerbation experiments, 10 µg of HDM, 150 µg of DEP, or a mixture of HDM and DEP were delivered intratracheally on days 0, 7, 8, or 9. Mice were humanely killed on day 10; then 100 µg of GSK484 (Cayman Chemicals, Ann Arbor, Mich) and/or 20 µg of montelukast (Cayman Chemicals) were delivered intratracheally on days 0, 7, 8, and 9 simultaneously. To induce ovalbumin (OVA)-induced asthma, mice were sensitized with 50 µg of OVA in 2 mg of alum intraperitoneally on days 0 and 10. Then mice were exposed to intratracheal antigens (30 µg of OVA per day) or phosphate-buffered saline (PBS) on days 14 and 17. For the OVA asthma exacerbation model, 20 µg of OVA, 150 µg of DEP, or a mixture of OVA and DEP was delivered

intratracheally on days 0, 7, 8, and 9, and mice were humanely killed on day 10. In the lipopolysaccharide (LPS)-induced lung injury model, mice were instilled with 5 µg of LPS for 3 consecutive days and humanely killed on the day after the last challenge. To investigate the *in vivo* effect of extracellular adenosine triphosphate (ATP), 50 µL of 100 mmol ATP (Sigma-Aldrich, St Louis, Mo) was instilled for 3 consecutive days.

### Measurement of AHR

Mice were anesthetized with 150 mg/kg of pentobarbital sodium. Tracheas were dissected, intubated with 18-gauge catheters, and mechanically ventilated at a tidal volume of 0.25 mL and a frequency of 140 breaths per minute. Respiratory system resistance ( $R_L$ ) was measured using invasive BUXCO FinePointe Resistance and Compliance (BUXCO Electronics, Wilmington, NC) in response to increasing doses (5, 10, 20, 40, 60 mg/mL) of aerosolized acetyl-β-methylcholine (methacholine) (Sigma-Aldrich). The average airway resistance was calculated for each methacholine concentrations and normalized to the saline.

### Histologic analysis

Lung tissues were fixed with 4% of paraformaldehyde (Biosesang, Seongnam, Republic of Korea) and embedded in paraffin. Paraffin blocks were cut into 4 µm thick sections and stained with hematoxylin and eosin. The extent of emphysema was measured by the mean linear intercept.<sup>23</sup> In brief, 5 fields for each sample were acquired randomly at a magnification of ×100, then overlaid with 50 × 50 µm grid using ImageJ software (National Institutes of Health, Bethesda, Md; <https://imagej.nih.gov/ij/>). The mean linear intercept value was calculated by dividing the total length of a line in the grid by the total alveolar wall intercepts.

### Flow cytometry

Lung was dissected, minced, incubated in RPMI 1640 media supplemented with 10% fetal bovine serum, 10 µg/mL of gentamycin, and 100 mg/mL collagenase IV (Worthington Biochemical, Lakewood, NJ) for 90 minutes and treated with RBC Lysis Buffer (BioLegend, San Diego, Calif). Single cells from the lung were suspended in PBS and stained using the Zombie Aqua Fixable Viability Kit (BioLegend) to exclude dead cells. After washing, cells were resuspended in fluorescence-activated cell sorting (FACS) buffer (PBS containing 2% bovine calf serum), blocked with anti-CD16/CD32 antibodies (BD Bioscience, Franklin Lakes, NJ), and stained with fluorochrome-labeled monoclonal antibodies against proper cell surface markers for 30 minutes at 4°C. For intracellular staining, the Fixation/Permeabilization Solution Kit with BD GolgiPlug (BD Bioscience) was used following the manufacturer's protocol. For staining of mouse immune cells, the following fluorochrome-labeled antibodies were used: anti-CD45 (30-F11), anti-CD3e (145-2C11), anti-CD11c (HL3), anti-CD11b (M1/70), anti-CD19 (ID3), anti-CD49b (DX5), anti-FceRIα (MAR-1), anti-CD90.2 (30-H12), anti-F4/80 (BM8), anti-Ly6G (1A8), anti-I-A<sup>b</sup> (AF6-120.1), anti-CD117 (2B8), anti-CD64L (MEL-14), anti-CXCR2 (SA044G4), anti-CXCR4 (L276F12), anti-Ly6C (HK1.4), anti-NK1.1 (PK136), anti-IL-5 (TRFK5), and anti-IL-17A (TC11-18H10.1) (all from BioLegend). Anti-SiglecF (E50-2440, from BD Bioscience), anti-IL-13 (eBio13A, from Thermo Fisher Scientific, Waltham, Mass), dihydrorhodamine 123 (Sigma-Aldrich). Alexa Fluor 647 donkey anti-rabbit IgG Abs (Thermo Fisher Scientific) was used as a secondary antibody for anti-P2X1 (polyclonal, Thermo Fisher Scientific). For staining of human cells from peripheral blood and induced sputum, single-cell suspensions were stained with the following antibodies: anti-CD16 (3G8), anti-CD24 (ML5), anti-CD206 (15-2), anti-CD15 (W6D3), anti-CD68 (Y1/82A), anti-Siglec8 (7C9), and anti-CD45 (HI30, BD Bioscience). All antibodies were purchased from BD Bioscience except for anti-CD45 Ab.

Data were collected on an LSRII Fortessa X-20 device (BD Bioscience) and analyzed by FlowJo v10.2 software (Treestar, Ashland, Ore). For visual stochastic network embedding (viSNE) and self-organizing maps (FlowSOM) analyses, data were analyzed using Cytobank.<sup>24</sup>

## RNA sequencing and data analysis

Eosinophils, conventional neutrophils, and SiglecF<sup>+</sup> neutrophils were sorted from lungs treated with DEP for 3 consecutive days. The total RNA of  $10^6$  cells of each population was extracted using the RNeasy Micro Kit (Qiagen, Germantown, Md). Quality control and subsequent RNA sequencing were carried out in the Laboratory of System Genomics, Pohang University of Science and Technology, Pohang, Republic of Korea. Briefly, mRNA was purified from total RNA with NEXTflex Poly(A) Beads (Bioo Scientific, Austin, Tex). The library of each sample was prepared for sequencing using the NEXTflex Rapid Directional RNA-Seq Kit (Bioo Scientific) and sequenced on a HiSeq2500 device (HiSeq 2500 platform; Illumina, San Diego, Calif) using the TruSeq Rapid SBS Kit (Illumina). On average, 60 million paired-end 100 bp reads were generated from each sample. For normalization, the transcripts per million was used. The RNA-Seq data were deposited in the Gene Expression Omnibus database (GSE158040) of the National Center for Biotechnology Information.

A Venn diagram was depicted with significant differential expressed genes that met a cutoff of 5% false discovery rate and 4-fold up- or downregulation among eosinophils, conventional neutrophils, and SiglecF<sup>+</sup> neutrophils. On the basis of significant differential expressed genes, Gene Ontology (GO; <http://geneontology.org/>) enrichment analysis and ClueGO analysis were performed. The relative expression level of the heat map was calculated as the z score.

## Proteome profile array

Proteins were extracted from 2 replicates of 6% DMSO-treated lungs and DEP-treated lungs, respectively, using 1% Triton X-100 (Biosesang) and proteinase inhibitor cocktail (Sigma-Aldrich). Proteome array was performed using Mouse XL Cytokine Array Kit (R&D Systems, Minneapolis, Minn) according to the manufacturer's instructions. Then spot intensities were calculated and normalized to reference spots. Protein expression levels were described as relativity to spot the intensity of the DMSO group in the heat map. Analysis was performed with an Amersham Imager 600 (Amersham Pharmacia Biotech, Piscataway, NJ) and ImageQuant TL software (GE Healthcare Life Science, Chicago, Ill).

## Cell morphology and immunofluorescence staining

To determine the morphology of eosinophils, conventional neutrophils, and SiglecF<sup>+</sup> neutrophils, each population was FACS sorted, spun on a cytocentrifuge (Thermo Shandon Cytopsin 4, Thermo Fisher Scientific), and stained with Diff-Quik solution (Sysmex, Kobe, Japan).

For immunofluorescence (IF) staining of SiglecF<sup>+</sup> neutrophils, BAL fluid extracted from DEP-exposed lungs were cytospan and stained with rat anti-mouse SiglecF (E50-2440; BD Bioscience) and goat polyclonal anti-human/mouse myeloperoxidase (MPO) polyclonal IgG (R&D Systems) and rabbit polyclonal anti-human/mouse histone H3 (citrulline R2 + R8 + R17; Abcam, Cambridge, United Kingdom) for 2 hours at room temperature. After several washes with PBS containing 0.05% Tween 20 (PBS-T), slides were stained with secondary antibodies including Alexa Fluor 594 donkey anti-rat IgG (Thermo Fisher Scientific), Alexa Fluor 488 donkey anti-goat IgG Abs (Thermo Fisher Scientific), and Alexa Fluor 647 donkey anti-rat IgG Abs (Abcam) for 1 hour at room temperature, followed by washing with PBS-T. Pro-Long Diamond Antifade Mountant with 4',6-diamidino-2-phenylindole (Thermo Fisher Scientific) was used to mount slides. Images were captured with a confocal microscope (A1 HD25; Nikon, Tokyo, Japan) and analyzed with NIS-Element Viewer imaging software (Nikon).

## Western blot analysis

Sorted conventional and SiglecF<sup>+</sup> neutrophils or lungs were lysed using radioimmunoprecipitation assay buffer (Biosesang) containing 0.15 mol sodium chloride, 1% Triton X-100, 1% sodium deoxycholate, 0.1% sodium dodecyl sulfate, 50 mmol Tris-HCl, and 2 mmol EDTA in the presence of protease inhibitor cocktails. An equivalent amount of protein per sample was loaded for

sodium dodecyl sulfate–polyacrylamide gel electrophoresis (12%) and electroblotted on polyvinylidene fluoride membranes. The membranes were blocked for 1 hour at room temperature with 5% of dry milk in Tris-buffered saline–Tween 20 (0.05%) and incubated overnight at 4°C with antibodies to CitH3 (rabbit polyclonal anti-Cit H3; 1:2000, Abcam) or P2X1 receptor (rabbit polyclonal anti-P2X1; 1:2000, Thermo Fisher Scientific). The membranes were then incubated for 1 hour at room temperature with appropriate horseradish peroxidase-conjugated secondary antibodies in Tris-buffered saline–Tween 20 (0.05%). Equal loading was confirmed by probing for β-actin (rabbit monoclonal anti-β-actin; 1:2000, Thermo Fisher Scientific).

## ELISA for lipid mediators, double-stranded DNA, and extracellular ATP

Sorted neutrophils was stimulated with 100 ng/mL of phorbol 12-myristate 13-acetate (Sigma-Aldrich) and 1 μg/mL of ionomycin (Sigma-Aldrich) for 2 hours at 37°C, and culture supernatants were collected for ELISA. The CysLT (Enzo Life Sciences, Farmingdale, NY) and prostaglandin D<sub>2</sub> (PGD<sub>2</sub>; Cusabio Technology, Houston, Tex) ELISAs were performed following the manufacturer's instructions. To measure the concentration of extracellular ATP, lung homogenate was used (adenosine triphosphate ELISA Kit; Aviva Systems Biology, San Diego, Calif). The concentration of double-stranded DNA (dsDNA) in the BAL fluid was measured using Quant-iT PicoGreen dsDNA reagent (Thermo Fisher Scientific) following the manufacturer's protocol.

## Quantitative real-time PCR

Murine neutrophils and isolated human polymorphonuclear neutrophil cells were homogenized with TRIzol reagent (Invitrogen/Thermo Fisher Scientific) with a BioMasher II. Total RNA was extracted, and cDNA was synthesized using the SensiFAST cDNA Synthesis kit (Bioline, London, United Kingdom). The expression levels of *Ltc4s* (leukotriene C<sub>4</sub> synthase), *Calm1*, *Calm2*, *Cherp*, *Camkk2*, *Gapdh*, *LTC4S*, and *RPLPO* were measured using a CFX Connect Real-Time PCR Detection System (Bio-Rad, Hercules, Calif). All primers were purchased from Integrated DNA Technologies (Coralville, Iowa). Relative expression levels were calculated as  $2^{-\Delta\Delta Ct}$  normalized to the expression of glyceraldehyde-3-phosphate dehydrogenase (*Gapdh*) and 60S acidic ribosomal protein P0 (*RPLPO*) for murine and human samples, respectively.

## Adoptive transfer of SiglecF<sup>+</sup> neutrophils

DEP-treated murine lungs were digested and stained with anti-CD45, anti-CD11b, anti-Ly6G, and anti-SiglecF. SiglecF<sup>+</sup> neutrophils were defined as the CD45<sup>+</sup>CD11b<sup>+</sup>Ly6G<sup>+</sup>SiglecF<sup>+</sup>SSC<sup>low</sup> population, and conventional neutrophils were defined as the CD45<sup>+</sup>CD11b<sup>+</sup>Ly6G<sup>+</sup>SiglecF<sup>-</sup>SSC<sup>low</sup> population. Each population of neutrophils was sorted using the BD FACSaria platform. The purity of sorted neutrophils was >95%. For asthmatic mice, more than  $2.5 \times 10^5$  cells of conventional or SiglecF<sup>+</sup> neutrophils were adoptively transferred intratracheally into the HDM treated recipient on day 8 and humanely killed on day 9. For naive mice,  $2.0 \times 10^6$  cells of conventional or SiglecF<sup>+</sup> neutrophils were adoptively transferred intratracheally into naive mice, which were humanely killed on day 7. To block CysLT secretion from SiglecF<sup>+</sup> neutrophils, SiglecF<sup>+</sup> neutrophils were pretreated with 10 μmol MK886 (Abcam) for 30 minutes at 37°C, washed with PBS 3 times, and transferred into asthmatic mice.

## Co-culture of neutrophils and T<sub>H</sub>2 cells

Naive CD4 T cells from wild-type C57BL/6 were sorted using MojoSort Mouse CD4 Naive T Cell Isolation Kit (BioLegend) following the manufacturer's protocol. Naive CD4 T cells ( $2 \times 10^5$  cells) were differentiated into T<sub>H</sub>2 cells using the CellXVivo mouse T<sub>H</sub>2 Cell Differentiation Kit (R&D Systems). Sorted conventional or SiglecF<sup>+</sup> neutrophils ( $2 \times 10^5$  cells) were added to differentiated T<sub>H</sub>2 cells on day 3, then analyzed on day 5.

## Co-culture of bone marrow neutrophils and DEP BAL or DEP-dissolved complete media

Bone marrow (BM)-derived neutrophils from wild-type C57BL/6 were isolated using a Neutrophil Isolation Kit following the manufacturer's protocol (Miltenyi Biotec, San Diego, Calif). BM neutrophil cells ( $3 \times 10^5$ ) were cultured with BAL extracted with 1 mL of complete RPMI 1640 media or DEP (50, 100, 200  $\mu\text{g}$ ) dissolved and sonicated with complete RPMI 1640 media for 48 hours. To inhibit P2X1 receptor signaling, NF449 was added during the culture at a final concentration of 50  $\mu\text{mol}$  for 48 hours.

## Human subjects and polymorphonuclear leukocyte isolation

Peripheral blood samples were obtained from 7 healthy controls and 26 patients with asthma (18 patients) or ACO (8 patients) from the Department of Internal Medicine, Seoul National University Hospital, Seoul, Republic of Korea. The criteria to divide the severity of asthma was the existence of chronic obstructive pulmonary disease. The demographics and disease severity of these groups are provided in Table E1 in this article's Online Repository at [www.jacionline.org](http://www.jacionline.org). All subjects enrolled onto this study gave written informed consent, and the study protocol was approved by the Seoul National University Hospital institutional review board (approval 1610-062-799).

Polymorphonuclear neutrophil cells were isolated as previously described.<sup>25</sup> Briefly, blood was gently layered over Histopaque 1119 (Sigma-Aldrich), then centrifuged at  $800 \times g$  for 25 minutes without braking. The reddish layer beneath the mononuclear cell layer was used for neutrophil experiments after red blood cell lysis.

## Statistical analysis

Comparisons of 2 groups were performed using an unpaired *t* test (parametric) or paired *t* test. Multiple groups were compared by 1-way ANOVA, followed by Tukey's *post hoc* multiple comparison (parametric). Correlations were determined by the Pearson correlation coefficient (parametric). Values represent the means  $\pm$  SEMs, and  $P < .05$  was considered statistically significant. Statistical analysis was performed by GraphPad Prism 7 software (GraphPad Software, La Jolla, Calif).

## RESULTS

### DEP exposure triggers the appearance of a distinct Ly6G<sup>+</sup> SiglecF<sup>+</sup> granulocyte population in the lungs

To examine the effects of air pollutants on the immune response in the airways, mice were exposed to DEP by intratracheal instillation for 3 consecutive days (Fig 1, A and B). This acute exposure induced mild airway inflammation and emphysema but no AHR. Proteome profile array analysis of the DEP-exposed and -unexposed lungs showed that DEP upregulated cytokines and molecules associated with neutrophil recruitment and function (CXCL5, CCL6, IL-17A, IL-1 $\alpha$ , TNF- $\alpha$ , and MPO) (Fig 1, C and D). When we analyzed the immune cells in the lung and in BAL fluid, both contained an unexpected population of granulocytes that expressed both Ly6G and SiglecF (Fig 1, E-G). The population emerged in a DEP dose-dependent manner (Fig E1, A). The number of SiglecF<sup>+</sup>Ly6G<sup>+</sup> granulocytes peaked on day 3 and disappeared 10 days after DEP exposure (Fig 1, H).

We then investigated whether other stimuli such as OVA and LPS, which respectively cause asthma and acute lung injury, can generate SiglecF<sup>+</sup>Ly6G<sup>+</sup> granulocytes *in vivo*. While intratracheal challenge with OVA and LPS respectively increased

eosinophil and neutrophil numbers in the lungs, both failed to induce SiglecF<sup>+</sup>Ly6G<sup>+</sup> granulocytes (Fig 1, I, and Fig E1, B-E). The DEP-induced SiglecF<sup>+</sup>Ly6G<sup>+</sup> granulocyte infiltration was limited to the lungs; these cells were not found in other tissues, including the mediastinal lymph nodes, blood, and BM (Fig 1, J). Ki-67 staining showed that the SiglecF<sup>+</sup>Ly6G<sup>+</sup> granulocytes are not actively proliferating (Fig 1, K). Therefore, we speculated that granulocytes that reside in lung tissue may acquire SiglecF expression upon DEP stimulation.

### SiglecF<sup>+</sup>Ly6G<sup>+</sup> granulocytes have unique features that distinguish them from other granulocytes

To further characterize the SiglecF<sup>+</sup>Ly6G<sup>+</sup> granulocytes, the immune populations in the lungs of DEP-exposed and -unexposed mice were subjected to unsupervised clustering. Again, only the DEP-exposed lungs contained high numbers of this SiglecF-expressing population; Fig 2, A, shows this population surrounded by a dashed line and located just adjacent to cluster 1, which contains neutrophils (Fig 2, A). We then wondered whether these SiglecF<sup>+</sup>Ly6G<sup>+</sup> granulocytes differ from other granulocytes. In terms of cell morphology and forward/side scatter profiles, the SiglecF<sup>+</sup>Ly6G<sup>+</sup> granulocytes were similar to neutrophils but differed from other SiglecF-expressing myeloid cell types, including eosinophils and alveolar macrophages in the DEP-exposed lung (Fig 2, B, and Fig E1, F). This identity as a neutrophil was supported by IF staining, which showed that SiglecF<sup>+</sup>Ly6G<sup>+</sup> granulocytes from DEP-exposed BAL fluid coexpressed the neutrophil granule constituent MPO and SiglecF (Fig 2, C). Additional experiments then confirmed that these cells are not eosinophils. First, although SiglecF<sup>+</sup>Ly6G<sup>+</sup> granulocytes were found to express a high level of SiglecE, similar to neutrophils, they did not express the eosinophil chemokine receptor CCR3 (Fig 2, D). Second, when  $\Delta$ dbleGATA mice, in which the eosinophil lineage is completely ablated,<sup>26</sup> were exposed to DEP intratracheally, the SiglecF<sup>+</sup>Ly6G<sup>+</sup> granulocytes were again observed in the lungs (Fig 2, E). Third, the transcriptomes of eosinophils, conventional neutrophils, and SiglecF<sup>+</sup>Ly6G<sup>+</sup> granulocytes from DEP-exposed lungs showed that 640 genes were upregulated in both neutrophils and SiglecF<sup>+</sup>Ly6G<sup>+</sup> granulocytes, but only 91 genes were upregulated in both eosinophils and SiglecF<sup>+</sup>Ly6G<sup>+</sup> granulocytes (Fig 2, F).

A closer look at the transcriptome data showed that 162 genes were upregulated in the SiglecF<sup>+</sup>Ly6G<sup>+</sup> granulocytes, but not the eosinophils or conventional neutrophils. These genes are related to immune cell migration, vasoconstriction, and cell-matrix adhesion. Indeed, none related to eosinophil activation (Fig 2, F-H). To obtain deeper insight into the development and function of SiglecF<sup>+</sup>Ly6G<sup>+</sup> granulocytes, we produced a volcano plot comparing the transcriptomes of conventional neutrophils and SiglecF<sup>+</sup>Ly6G<sup>+</sup> granulocytes (Fig 2, I). The gene networks that were upregulated in SiglecF<sup>+</sup>Ly6G<sup>+</sup> granulocytes relative to the conventional neutrophils were determined by using ClueGO,<sup>27</sup> a plug-in for Cytoscape that creates functional groups by integrating GO terms (Fig 2, J).<sup>28</sup> These gene networks are related to the regulation of smooth muscle contraction, protein processing, and purinergic nucleotide receptor signaling.

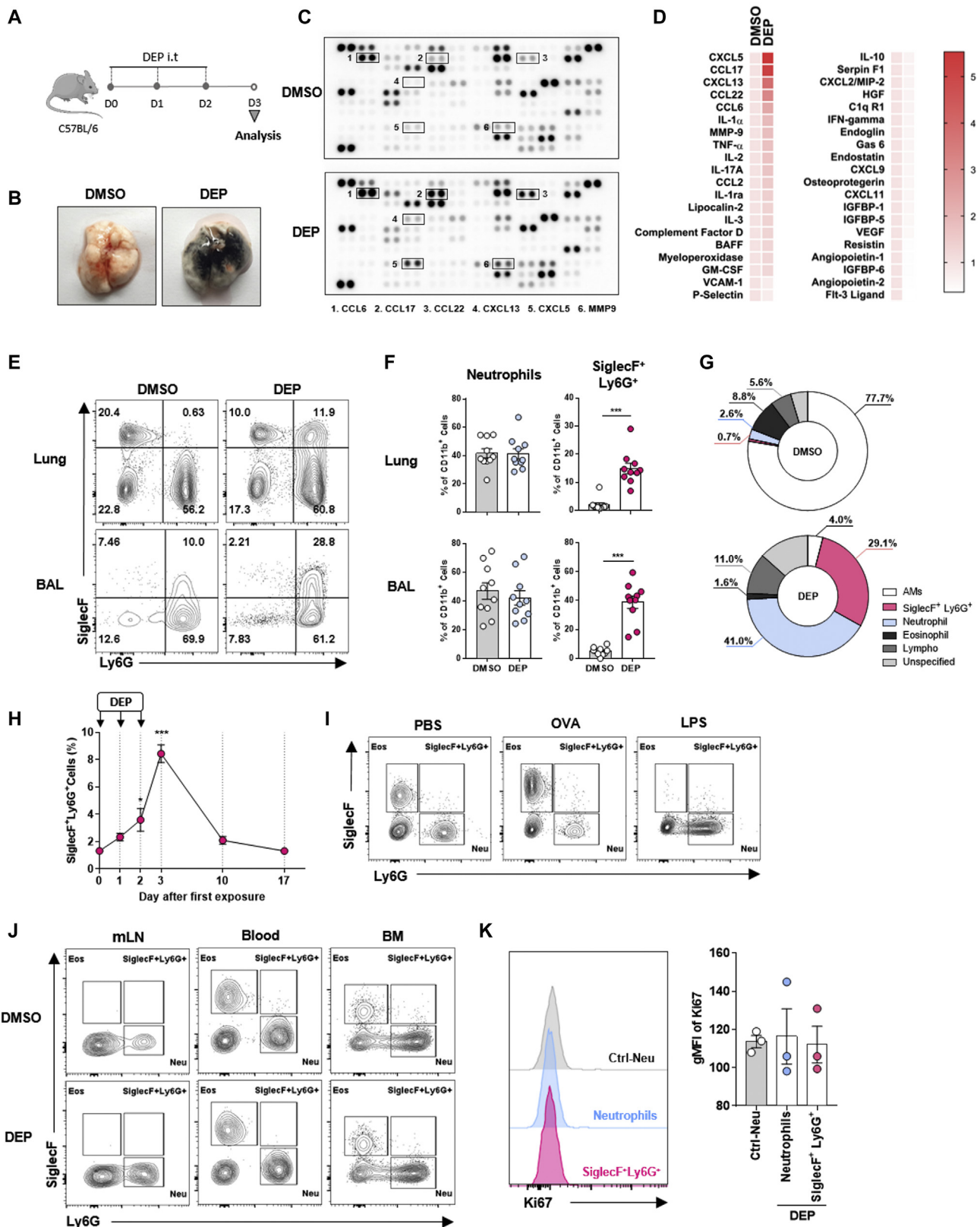


**FIG 1.** SiglecF<sup>+</sup>Ly6G<sup>+</sup> granulocytes appeared exclusively in DEP-exposed lungs. **A**, Experimental protocol of DEP exposure. **B**, Representative lung images of DMSO- or DEP-exposed mice. **C, D**, Proteome profiler cytokine array of DMSO- and DEP-treated lungs. At left are representative spots of neutrophil attractant chemokines; at right, heat map of top-ranked and bottom-ranked 20 cytokines ( $n = 2$  per group). **E, F**, Frequencies of granulocytes of both lung and BAL fluid from DMSO- or DEP-treated mice ( $n = 10$  per group). **G**, Percentage distribution of cell types in DMSO and DEP lungs. **H**, Kinetics of SiglecF<sup>+</sup>Ly6G<sup>+</sup> cell appearance in DEP-exposed mice. **I**, Flow cytometry analysis of PBS, OVA, and LPS-treated mice. **J**, Flow cytometry analysis of mLN, blood, and BM. **K**, Histogram of Ki67 expression in Ctrl-Neu and Neutrophils, with a bar graph of gMFI of Ki67 for Ctrl-Neu, Neutrophils, and SiglecF<sup>+</sup> Ly6G<sup>+</sup>.

Thus, the surface marker, morphology, and sequencing data together suggest that SiglecF<sup>+</sup>Ly6G<sup>+</sup> granulocytes are a new subset of neutrophils that have a unique transcriptome. Henceforth, SiglecF<sup>+</sup>Ly6G<sup>+</sup> granulocytes will be referred to as SiglecF<sup>+</sup> neutrophils.

### Purinergic receptor signaling is required to induce SiglecF expression by neutrophils

To determine how DEP induces the expression of SiglecF on neutrophils, we cultured BM-derived neutrophils with either DEP or BAL fluid from DEP-exposed mice (DEP BAL). Direct exposure to DEP only slightly increased the SiglecF expression of the neutrophils (Fig 3, A), and SiglecF expression was not further upregulated by increasing dose (see Fig E2, A and B, in this article's Online Repository at [www.jacionline.org](http://www.jacionline.org)) and incubation time of DEP (Fig E2, E and F). By contrast, the BAL fluid from DEP-exposed mice greatly increased neutrophil expression of SiglecF in a dose- and a time-dependent manner (Fig 3, B, and Fig E2, C and D, and G and H). Therefore, soluble factor or factors in the lung induced by DEP exposure may generate SiglecF<sup>+</sup> neutrophils.

Because gene networks related to purinergic nucleotide receptor signaling, especially purinergic P2X1 receptor and calcium signaling-related gene expression, were increased in SiglecF<sup>+</sup> neutrophils (Fig 2, J, and Fig 3, C), we hypothesized that P2X1 receptor signaling could contribute to the generation of SiglecF<sup>+</sup> neutrophils. Flow cytometry of the neutrophils from DEP-treated lungs and western blot analysis of SiglecF<sup>+</sup> neutrophils from DEP-treated lung showed that the SiglecF<sup>+</sup> neutrophils expressed higher levels of the P2X1 receptor compared to conventional neutrophils (Fig 3, D and E). Calcium signaling-related genes (*Calm1*, *Calm2*, *Cherp*, and *Camkk2*) were also upregulated in neutrophils cultured with DEP BAL, but not DEP media (Fig E2, I). *In vitro* blockade of the P2X1 receptor with the selective antagonist NF449<sup>29</sup> reduced the SiglecF expression of DEP BAL-treated neutrophils (Fig 3, F). Consistently, the lungs of DEP-exposed mice had higher levels of extracellular ATP, which is a danger signal that activates the P2X1 receptor (Fig 3, G).<sup>30</sup> Finally, administration of ATP into the naive mice resulted in the generation of SiglecF<sup>+</sup> neutrophils *in vivo* (Fig 3, H and I). These findings show that DEP-mediated induction of SiglecF expression on neutrophils in the lung may involve P2X1 receptor signaling in these cells, and that DEP achieves this effect indirectly, possibly by inducing extracellular ATP or other P2X1 receptor-activating danger signals.

### SiglecF<sup>+</sup> neutrophils have greater NET-forming capacity than conventional neutrophils

We next investigated the functional differences between conventional and SiglecF<sup>+</sup> neutrophils derived from the DEP-exposed lung. The RNA-Seq data showed that SiglecF<sup>+</sup>

neutrophils expressed genes related to protein processing (eg, *Mmp14*, *Plau*, *Cldn1*, and *Timm17a*) and NET formation (eg, *Atk*, *Mtor*, *Map3K*, and *Ctsa*) at higher levels than conventional neutrophils (Fig 4, A and B). IF staining of DEP-exposed and -unexposed lungs showed that DEP not only increased the number of SiglecF and Ly6G coexpressing cells (as shown in Fig 2, C) but also that these cells coexpressed the NET component CitH3 (Fig 4, C). Western blot analysis confirmed that SiglecF<sup>+</sup> neutrophils from the DEP-exposed lung had higher CitH3 protein levels than conventional neutrophils (Fig 4, D). Moreover, flow cytometry showed that the SiglecF<sup>+</sup> neutrophils had higher levels of reactive oxygen species (ROS), as measured by staining the cells with dihydrorhodamine 123 (Fig 4, E and F). This is significant because neutrophil ROS drive NET formation.<sup>31,32</sup> Unlike DEP-induced SiglecF<sup>+</sup> neutrophils, no significant increases in the levels of ROS and CitH3 were observed in ATP-induced SiglecF<sup>+</sup> neutrophils (see Fig E3, A and B, in this article's Online Repository at [www.jacionline.org](http://www.jacionline.org)), implying that ATP alone is insufficient for NET formation in SiglecF<sup>+</sup> neutrophils. Moreover, when SiglecF<sup>+</sup> neutrophils were cultured and observed over time, they produced NETs in the absence of any stimulation; conventional neutrophils did not generate NETs (Fig 4, G). Thus, DEP-induced SiglecF<sup>+</sup> neutrophils are more prone to producing NETs than conventional neutrophils.

Several studies have shown that patients with chronic obstructive pulmonary disease, including emphysema and chronic bronchitis, have increased NET formation in their sputum.<sup>33,34</sup> Because mice that were exposed intratracheally to DEP exhibited emphysema, we wondered whether the NET-prone SiglecF<sup>+</sup> neutrophils in DEP-treated mice contributed to emphysema. For this, we simultaneously treated the mice with DEP and GSK484, an inhibitor of NET formation (Fig 4, H).<sup>35</sup> Indeed, inhibiting NET formation significantly reduced DEP-induced emphysema (Fig 4, I and J). It also reduced the expression of not only CitH3 but also IL-17A in the lung (Fig E3, C-F). Notably, when naive mice received SiglecF<sup>+</sup> neutrophils by intratracheal adoptive transfer, they developed emphysema; conventional neutrophils did not have this effect (Fig 4, K-M). Thus, the enhanced NET-forming ability of SiglecF<sup>+</sup> neutrophils can mediate the development of DEP-induced emphysema, possibly by activating type 3 immune responses.

### SiglecF<sup>+</sup> neutrophils exacerbate asthma by secreting CysLTs

As shown in Fig 2, J, gene sets that relate to airway smooth muscle constriction are upregulated in SiglecF<sup>+</sup> neutrophils. These genes encode enzymes that are essential for the synthesis of lipid mediators of inflammation. They include *Ptgs1*, which encodes prostaglandin H<sub>2</sub>, a precursor of other prostaglandins, including PGD<sub>2</sub>; *Ltc4s*, which encodes the leukotriene C<sub>4</sub> synthase enzyme that synthesizes CysLT, namely leukotriene C<sub>4</sub> (LTC<sub>4</sub>), leukotriene D<sub>4</sub>, and leukotriene E<sub>4</sub>; and *Cysltr1*, which

group). **G**, The numerical proportion of BAL immune cell populations. **H**, Frequencies of lung SiglecF<sup>+</sup>Ly6G<sup>+</sup> granulocytes after DEP treatment (n = 3 per each time point). **I**, Representative dot plot of SiglecF<sup>+</sup>Ly6G<sup>+</sup> granulocytes in the lungs from OVA- and LPS-treated mice. **J**, Representative dot plots of SiglecF<sup>+</sup>Ly6G<sup>+</sup> granulocytes in mediastinal lymph nodes (mLN), blood, and BM. **K**, Ki-67 expression of neutrophils and SiglecF<sup>+</sup>Ly6G<sup>+</sup> granulocytes from naive and DEP-exposed mice (n = 3 per group). Data are pooled from 2 or 3 independent experiments (E-G) or are representative of 3 independent experiments (A-D, H-K) with values represented as means ± SEMs. \*P < .05, \*\*P < .001.

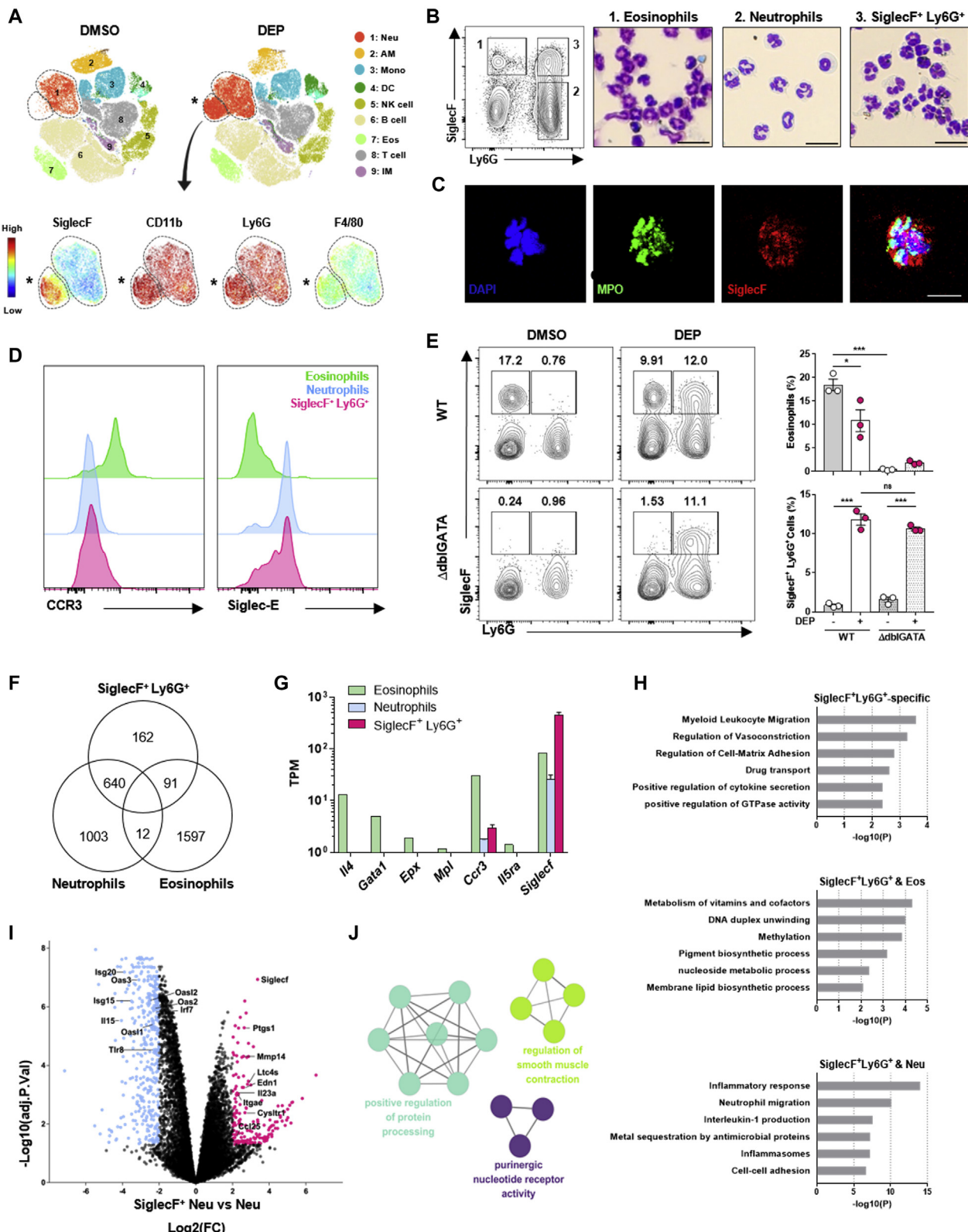


**FIG 2.** SiglecF<sup>+</sup>Ly6G<sup>+</sup> granulocytes were distinct from conventional neutrophils and eosinophils. **A**, tSNE plots merged with viSNE and FlowSOM analysis. The dashed line indicates neutrophils; asterisk, SiglecF<sup>+</sup>Ly6G<sup>+</sup> granulocytes. **B**, Representative cytopsin images of granulocytes from DEP-treated lungs. Scale bar = 25  $\mu$ m. **C**, IF image of SiglecF<sup>+</sup>Ly6G<sup>+</sup> granulocytes. Green indicates MPO; red, SiglecF; and blue, 4',6-diamidino-2-phenylindole. Scale bar = 25  $\mu$ m. **D**, Histogram of CCR3 and SiglecE expression of each population from DEP-exposed lungs. **E**, Dot plots and frequencies of eosinophils and SiglecF<sup>+</sup>Ly6G<sup>+</sup>

encodes the receptor for the CysLT (Fig 5, A, and see Fig E4, A, in this article's Online Repository at [www.jacionline.org](http://www.jacionline.org)). The PGD<sub>2</sub> and CysLT lipid mediators can induce and enhance type 2 inflammation and AHR.<sup>36</sup> Notably, sorted SiglecF<sup>+</sup> neutrophils from the DEP-exposed lung that were treated with phorbol 12-myristate 13-acetate/ionomycin produced significantly higher levels of CysLT than conventional neutrophils (Fig 5, B), although these levels were somewhat lower than the levels produced by eosinophils, a representative cellular source of CysLT (Fig E4, B). SiglecF<sup>+</sup> neutrophils did not produce more PGD<sub>2</sub> than conventional neutrophils (Fig 5, B). *In vitro*-generated SiglecF<sup>+</sup> neutrophils also expressed higher levels of *Ltc4s* (Fig 5, C). Moreover, DEP-exposed  $\Delta$ dblGATA mice had elevated levels of CysLTs in their BAL fluid (Fig E4, C). This extra CysLT was likely from SiglecF<sup>+</sup> neutrophils because when we analyzed the other cells that produce CysLTs (Fc $\epsilon$ RI $\alpha^+$  CD11b<sup>-</sup> cells and monocytes) in the DEP-exposed and -unexposed  $\Delta$ dblGATA mouse lungs, we observed that these populations were not affected by DEP exposure (Fig E4, D). Thus, SiglecF<sup>+</sup> neutrophils appear to be a novel cellular source of the CysLTs that are known to promote asthmogenic type 2 inflammation. This is further supported by experiments where naive CD4<sup>+</sup> T cells cultured under T<sub>H</sub>2-skewing conditions were co-cultured with SiglecF<sup>+</sup> neutrophils: SiglecF<sup>+</sup> neutrophils enhanced the type 2 cytokine (IL-5 and IL-13) production of the T cells (Fig 5, D-F).

Because CysLTs are well-known targets of asthma therapy, we next asked whether CysLTs from SiglecF<sup>+</sup> neutrophils could aggravate asthma. Indeed, when asthma was induced in naïve mice with HDM extract and sorted SiglecF<sup>+</sup> neutrophils were adoptively transferred intratracheally, the AHR and eosinophil infiltration was profoundly increased. In contrast, the transfer of conventional neutrophils did not have the same effect (Fig 5, G-I). The adoptive transfer of SiglecF<sup>+</sup> neutrophils also markedly increased the type 2 (IL-5 and IL-13) cytokines produced by both the CD4<sup>+</sup> T cells (Fig 5, J and K) and the ILC2s (Fig 5, L and M) from the lung of the asthmatic mice. We then asked whether MK886, which inhibits a 5-lipoxygenase-activating protein and disrupts CysLT production (Fig 5, N),<sup>37</sup> can impair the ability of adoptively transferred SiglecF<sup>+</sup> neutrophils to exacerbate asthma. Our initial experiment confirmed that MK886 sharply impaired the CysLT production of SiglecF<sup>+</sup> neutrophils *in vitro* (Fig 5, O). When MK886-treated SiglecF<sup>+</sup> neutrophils were transferred into asthmatic mice, the enhanced AHR was much less evident (Fig 5, P). Moreover, transfer of the MK886-treated SiglecF<sup>+</sup> neutrophils was associated with fewer IL-5<sup>+</sup> and IL-13<sup>+</sup> cells in the lung (Fig 5, Q). Like DEP-induced SiglecF<sup>+</sup> neutrophils, the level of *Ltc4s* expression was upregulated in ATP-induced SiglecF<sup>+</sup> neutrophils (Fig E4, E). Also, ATP-exposed mice contained higher levels of BAL CysLT (Fig E4, F). Thus, SiglecF<sup>+</sup> neutrophils can exacerbate asthma by secreting CysLTs and thereby enhancing type 2 inflammation and AHR.

## DEP-mediated exacerbation of asthma is associated with SiglecF<sup>+</sup> neutrophils

As in humans, when mice are exposed to the environmental pollutant DEP as well as an asthma trigger such as HDM, they developed more severe asthma.<sup>5</sup> We used an HDM + DEP-induced murine model to further elucidate how SiglecF<sup>+</sup> neutrophils exacerbate asthma (Fig 6, A). Mice treated with a suboptimal dose of HDM or DEP alone failed to develop AHR; however, combining HDM and DEP significantly increased AHR and eosinophil infiltration into the BAL fluid (Fig 6, B and C). In addition, lungs treated with both HDM and DEP had enlarged alveoli accompanied by inflammatory cell infiltration around the airways (Fig 6, D and E). As shown above, DEP but not HDM generated SiglecF<sup>+</sup> neutrophils; HDM + DEP yielded the same numbers as DEP alone (see Fig E5, A and B, in this article's Online Repository at [www.jacionline.org](http://www.jacionline.org)). Similarly, DEP but not HDM elevated the dsDNA levels in the BAL fluid; HDM + DEP treatment generated the same levels as DEP alone (Fig 6, F). The same pattern was observed for CysLTs in the BAL fluid (Fig 6, H). Notably, when the data of the DEP-alone and HDM + DEP-treated mice were pooled, both the concentrations of dsDNA and CysLT in the BAL fluid correlated positively with the percentage of SiglecF<sup>+</sup> neutrophils in the BAL fluid ( $r = 0.4559$  and 0.5263, respectively) (Fig 6, G and I). Moreover, HDM but not DEP elevated type 2 (IL-5 and IL-13) cytokine production by CD4<sup>+</sup> T cells in the BAL fluid; notably, adding DEP to HDM further increased these HDM-induced type 2 cytokines from T cells (Fig 6, J and K) and ILCs (Fig E5, C). While DEP and HDM both increased type 3 (IL-17A) responses by CD4<sup>+</sup> T cells (Fig 6, L), none of the treatments had any effect on type 3 immune responses by ILCs (Fig E5, D). Thus, combining HDM and DEP induced severe asthma that was accompanied by elevated SiglecF<sup>+</sup> neutrophil numbers, dsDNA (ie, NET), and CysLT levels in the BAL fluid.

To determine whether this phenomenon applies to another asthma model, we induced asthma by OVA administration instead of HDM using the same experimental protocol of the HDM + DEP model (see Fig E6, A, in this article's Online Repository at [www.jacionline.org](http://www.jacionline.org)). Mice treated with OVA or DEP alone did not develop AHR; however, the combination of OVA and DEP significantly increased AHR and eosinophil infiltration into the BAL fluid (Fig E6, B and C). SiglecF<sup>+</sup> neutrophils also developed in the OVA + DEP-exposed group (Fig E6, D). Moreover, neither DEP nor OVA alone increased cytokine production from T cells and ILCs, but the combination of DEP and OVA further increased both type 2 and type 3 cytokines from T cells and ILCs (Fig E6, E and F).

## Double blockade of NET and CysLT profoundly inhibits DEP-mediated exacerbation of asthma

We next asked whether the blockade of NET and CysLT production from SiglecF<sup>+</sup> neutrophils ameliorated HDM +

granulocytes in wild-type and  $\Delta$ dblGATA mice. F, Venn diagram showing the number of upregulated genes among 3 populations. G, Transcripts per million (TPM) of eosinophil-associated genes of each population. H, GO analysis of differentially expressed genes among 3 populations from DEP-exposed lungs. I, Volcano plot of comparative gene expression of neutrophils and SiglecF<sup>+</sup>Ly6G<sup>+</sup> granulocytes. J, ClueGO functional grouping of GO terms upregulated in SiglecF<sup>+</sup>Ly6G<sup>+</sup> granulocytes. Images are representative of 1 of 3 independent experiments (A-D). Data are representative of 3 independent experiments (E) with values represented as means  $\pm$  SEMs. \* $P < .05$ , \*\*\* $P < .001$ .

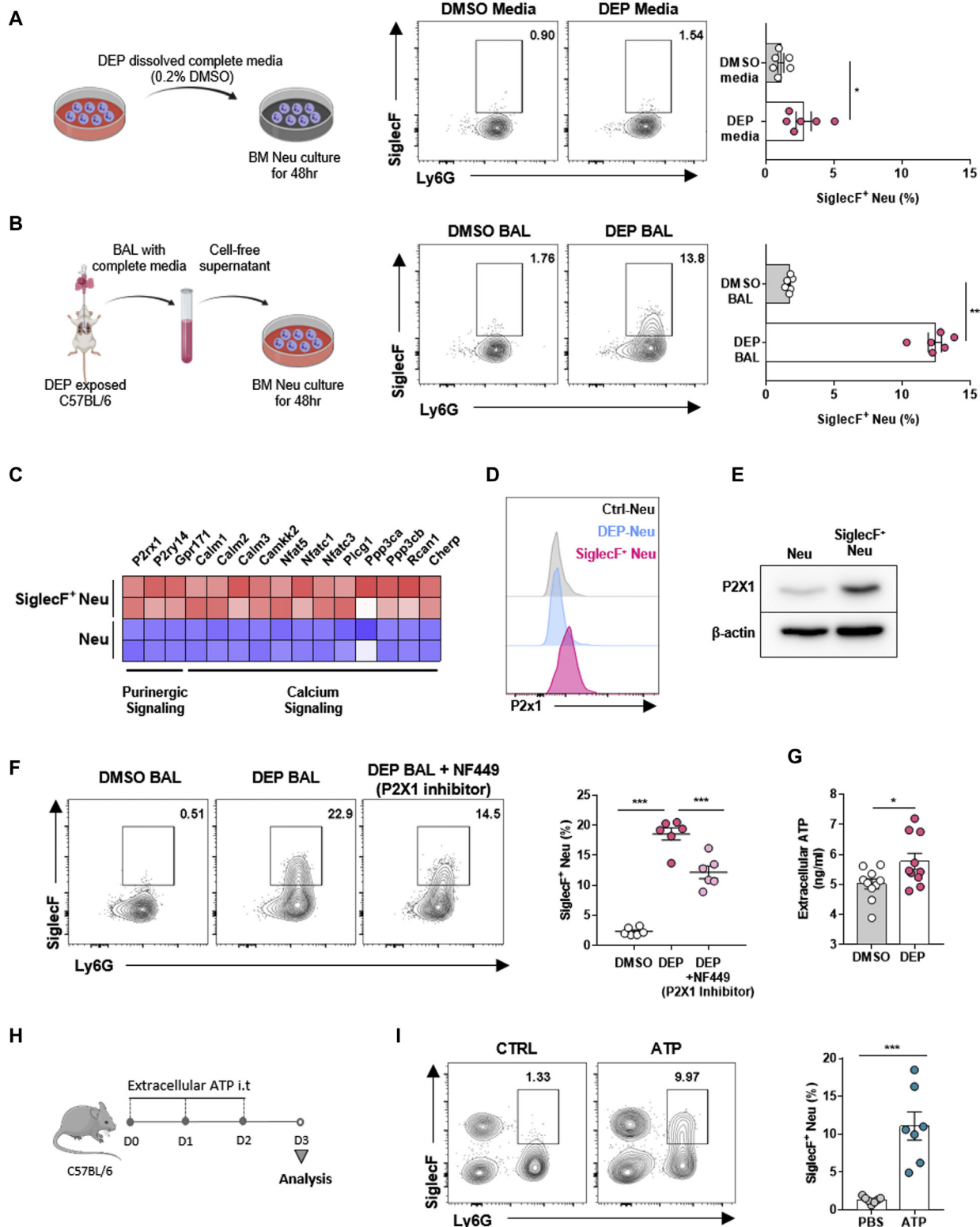


**FIG 3.** Extracellular P2X1 delivers signals for SiglecF expression on neutrophils. **A, B**, Dot plots and bar graphs of SiglecF expression of BM-derived neutrophils cultured with DEP (**A**) or BAL fluid obtained from DMSO- or DEP-treated mice (**B**). **C**, Heat map presenting z score of genes associated with purinergic receptor signaling and calcium signaling of each population from DEP-exposed lungs. **D**, Histogram of P2X1 receptor expression on neutrophils from naive mice (Ctrl-Neu), DEP-exposed neutrophils, and SiglecF<sup>+</sup> neutrophils. **E**, Western blot analysis of P2X1 receptor of each population from DEP-exposed lungs. **F**, BM-derived neutrophils cultured with DEP BAL with or without NF449 (n = 6 per group). **G**, ELISA of extracellular ATP in the DMSO- or DEP-exposed lungs (n = 10 per group). **H**, Experimental protocol of ATP exposure. **I**, Representative flow cytometric dot plot (*left*) and frequencies (*right*) of SiglecF<sup>+</sup> neutrophils from ATP-exposed mice. Data are representative of 3 independent experiments (**D, E**) or pooled in 2 independent experiments (**A, B, F-I**) with values represented as means  $\pm$  SEMs. \*P < .05, \*\*P < .01, \*\*\*P < .001.

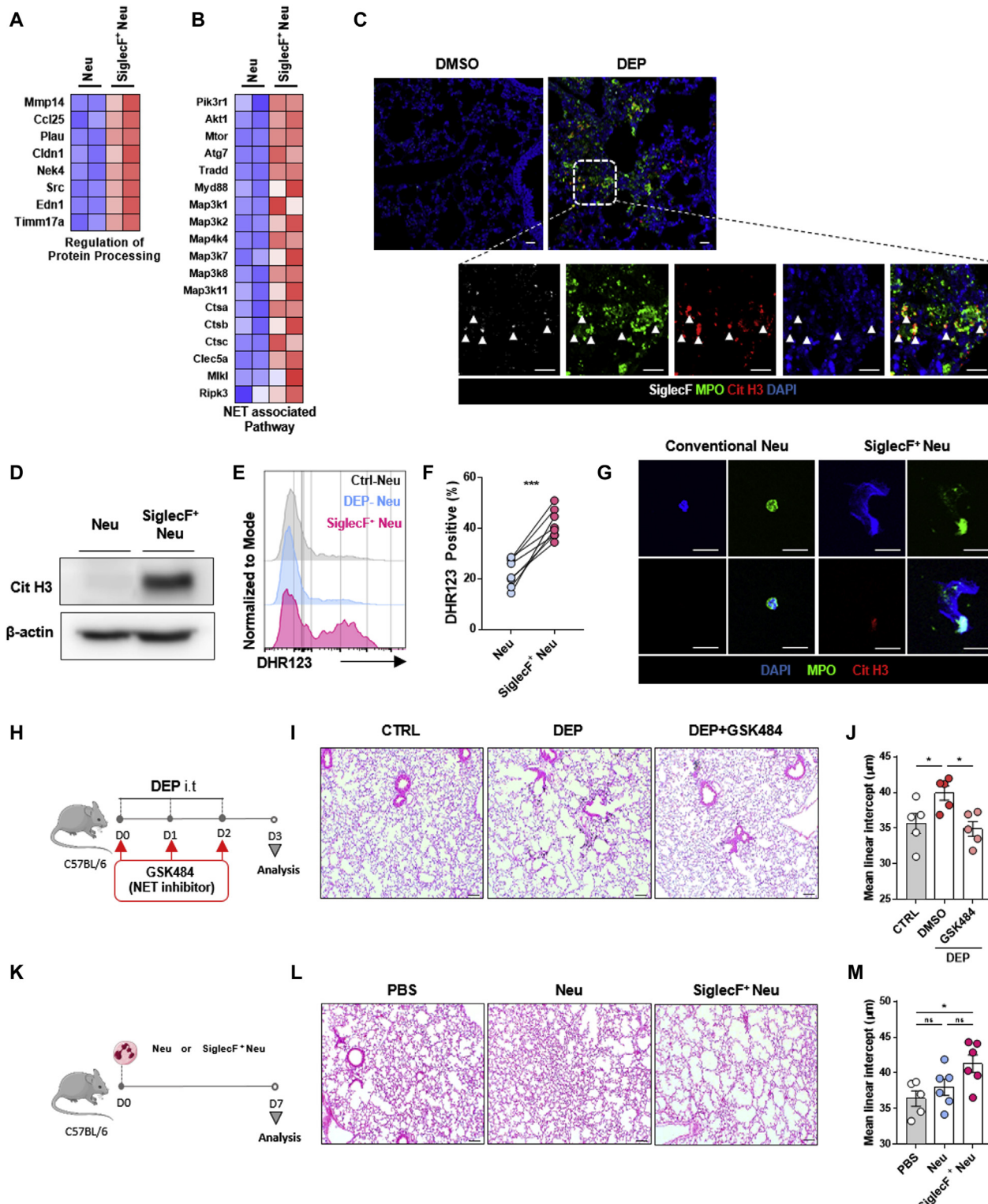


**FIG 4.** SiglecF<sup>+</sup> neutrophil trigger emphysema via NET formation. **A, B**, Heat map presenting zscore of genes associated with protein processing (**A**) and NET-associated pathway (**B**) of each neutrophil population. **C**, IF staining of DMSO- or DEP-exposed lungs. Scale bar = 20  $\mu$ m. **D**, Western blot analysis for NET-related CitH3 expression. **E, F**, Histogram (**E**) and paired graph (**F**) of dihydrorhodamine (DHR) 123 expressions in conventional or SiglecF<sup>+</sup> neutrophils ( $n = 8$  per group). **G**, IF staining of *ex vivo* NET formation. Scale bar = 20  $\mu$ m. **H**, Schematic diagram of GSK484 treatment during DEP exposure. **I**, Representative histology of each group. Scale bar = 100  $\mu$ m. **J**, Graph of mean linear intercept ( $n = 5$  per group). **K**, Experimental protocol of adoptive transfer. **L, M**, Representative histology and mean linear intercept of conventional or SiglecF<sup>+</sup> neutrophil transferred lungs. Scale bar = 100  $\mu$ m ( $n = 5\text{--}6$  for each group). Images are representative of 8 lungs from 3 independent experiments (**C**) or 5 or 6 lungs pooled from 3 independent experiments (**I, L**). Data are representative of 3 independent experiments (**D, G**) or pooled from 2 or 3 independent experiments (**E, F, H-M**) with values represented as means  $\pm$  SEMs. \* $P < .05$ , \*\* $P < .01$ , \*\*\* $P < .001$ .

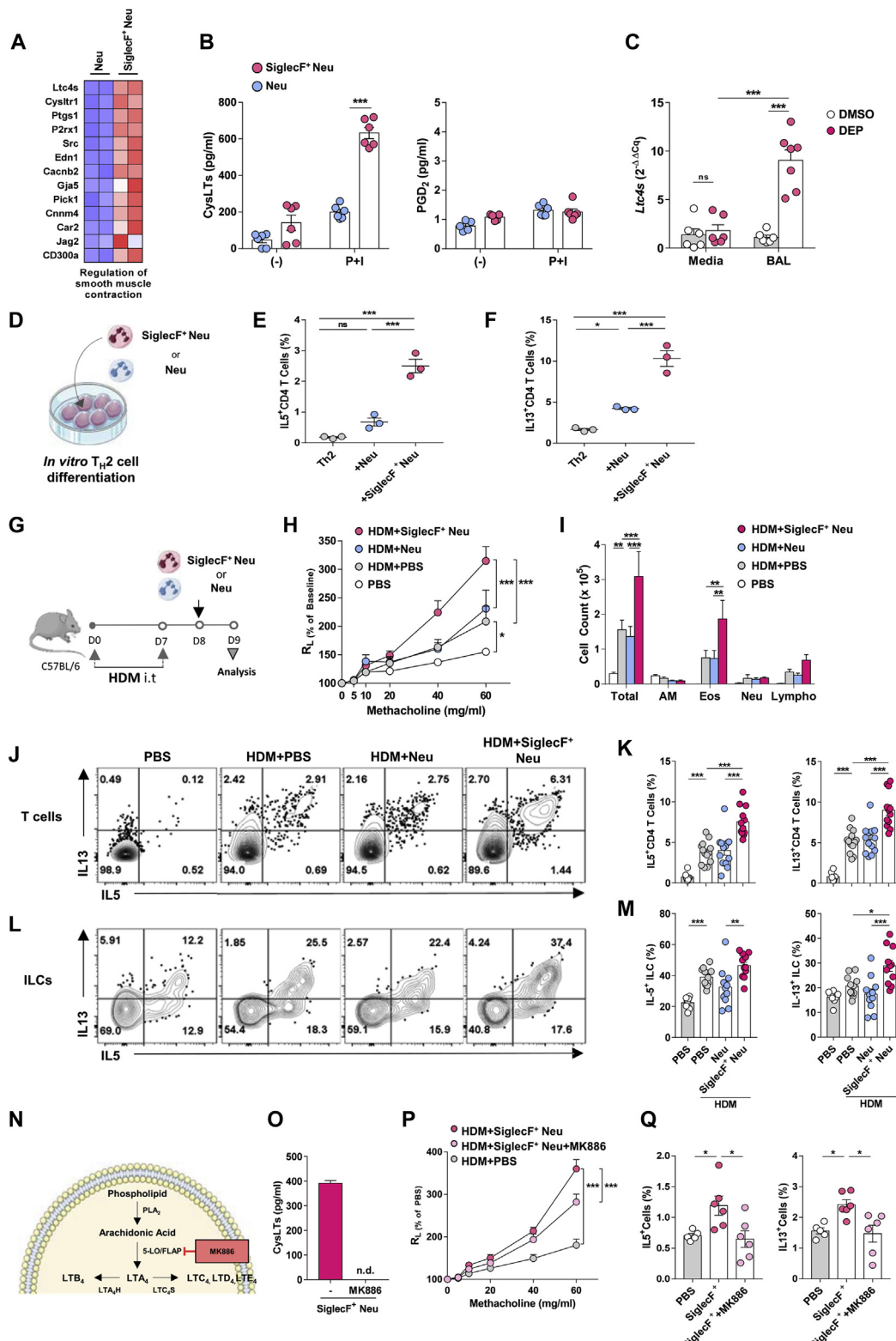


**FIG 5.** CysLTs secreted from SiglecF<sup>+</sup> neutrophils aggravate asthma. **A**, Heat map presenting genes associated with smooth muscle contraction. **B**, CysLT and PGD<sub>2</sub> levels of culture supernatants. **C**, Relative *Ltc4s* expression of cultured BM neutrophils depicted in Fig 3, A and B ( $n = 6$  per group). **D**, Co-culture protocol of T cells with each neutrophil subset. **E, F**, Frequencies of IL-5- and IL-13-positive T cells. **G**, Experimental protocol of adoptive transfer. **H, I**, AHR ( $H$ ) and differential BAL fluid immune cell counts ( $I$ ) of each group. **J-M**, Representative flow cytometric dot plots and bar graphs of IL-5- and IL-13-positive CD4 T cells ( $J, K$ ) and ILCs ( $L, M$ ) ( $n = 8-13$  for each group). **N**, Schematic diagram of the biochemical action of MK886. **O**, CysLT levels in vehicle- or MK886-treated SiglecF<sup>+</sup> neutrophils ( $n = 2$  per group). **P, Q**, AHR ( $P$ ) and frequencies of IL-5- and IL-13-positive cells ( $Q$ ) ( $n = 5-6$  for each group). Data are representative of 2 independent experiments (*D-F*) or pooled from 3 or 4 (*B, C, G-Q*) independent experiments with values represented as means  $\pm$  SEMs. \* $P < .05$ , \*\* $P < .01$ , \*\*\* $P < .001$ .

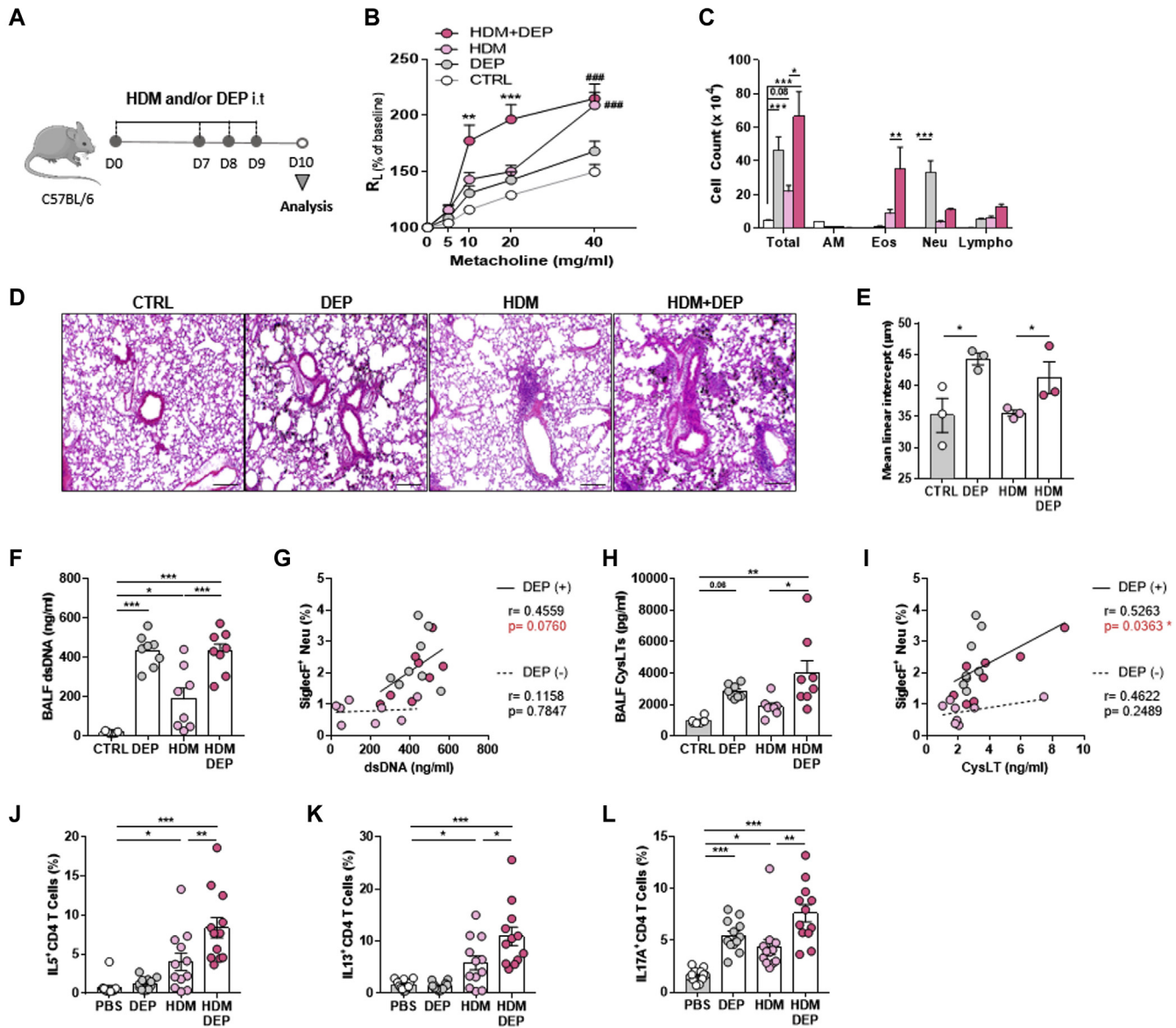


**FIG 6.** DEP-mediated exacerbation of allergic asthma is associated with SiglecF<sup>+</sup> neutrophils. **A**, Schematic diagram of HDM and DEP treatment. **B**, AHR of each group described in (A). **C**, Differential BAL fluid immune cell counts. **D**, **E**, Histology (D) and mean linear intercepts (E) of each group. **F**, **G**, dsDNA levels measured in BAL fluid of each group (F) and a correlation between the SiglecF<sup>+</sup> neutrophils and dsDNA levels (G). **H**, **I**, CysLT levels measured in BAL fluid of each group (H), and a correlation between SiglecF<sup>+</sup> neutrophils and CysLT levels (I). The solid line indicates the correlation in both the DEP and HDM + DEP merged groups; dashed line, correlation in the HDM group (F-I; n = 8 per group). **J-L**, Frequencies of IL-5<sup>+</sup> (J), IL-13<sup>+</sup> (K), and IL-17A<sup>+</sup> (L) positive CD4 T cells (n = 12 per group). Data are pooled from 2 or 3 independent experiments (B, C, F-L) with values represented as means  $\pm$  SEMs. \*P < .05, \*\*P < .01, \*\*\*P < .001.

DEP-induced asthma. To test this, mice were treated with either or both GSK484 (NET inhibitor) and montelukast (CysLT receptor 1 antagonist)<sup>38</sup> at HDM + DEP treatment (Fig 7, A). While either treatment alone significantly reduced the development of AHR, the NET inhibitor was particularly effective (Fig 7, B). However, only the 2 treatments together significantly reduced the total inflammatory cell and eosinophil counts in the BAL fluid (Fig 7, C). Notably, the NET inhibitor significantly increased the total inflammatory and neutrophil cell numbers in the BAL fluid. This appears to be due to the accumulation of SiglecF<sup>+</sup> neutrophils, which in the absence of NET inhibitor would otherwise

undergo NETosis-induced cell death (Fig 7, C and D). Most importantly, coadministration of NET inhibitor and CysLT receptor 1 antagonist tended to suppress the type 2 and 3 cytokine production in the BAL fluid more efficiently than either agent on its own (Fig 7, E-G). Therefore, targeting SiglecF<sup>+</sup> neutrophils could be an effective therapeutic strategy for patients with asthma with a mixed phenotype, which is a common characteristic in severe asthma.

Finally, we asked whether humans also bear SiglecF<sup>+</sup> neutrophil-type cells and whether these cells associate with the severity of asthma. Because Siglec8 is a functional

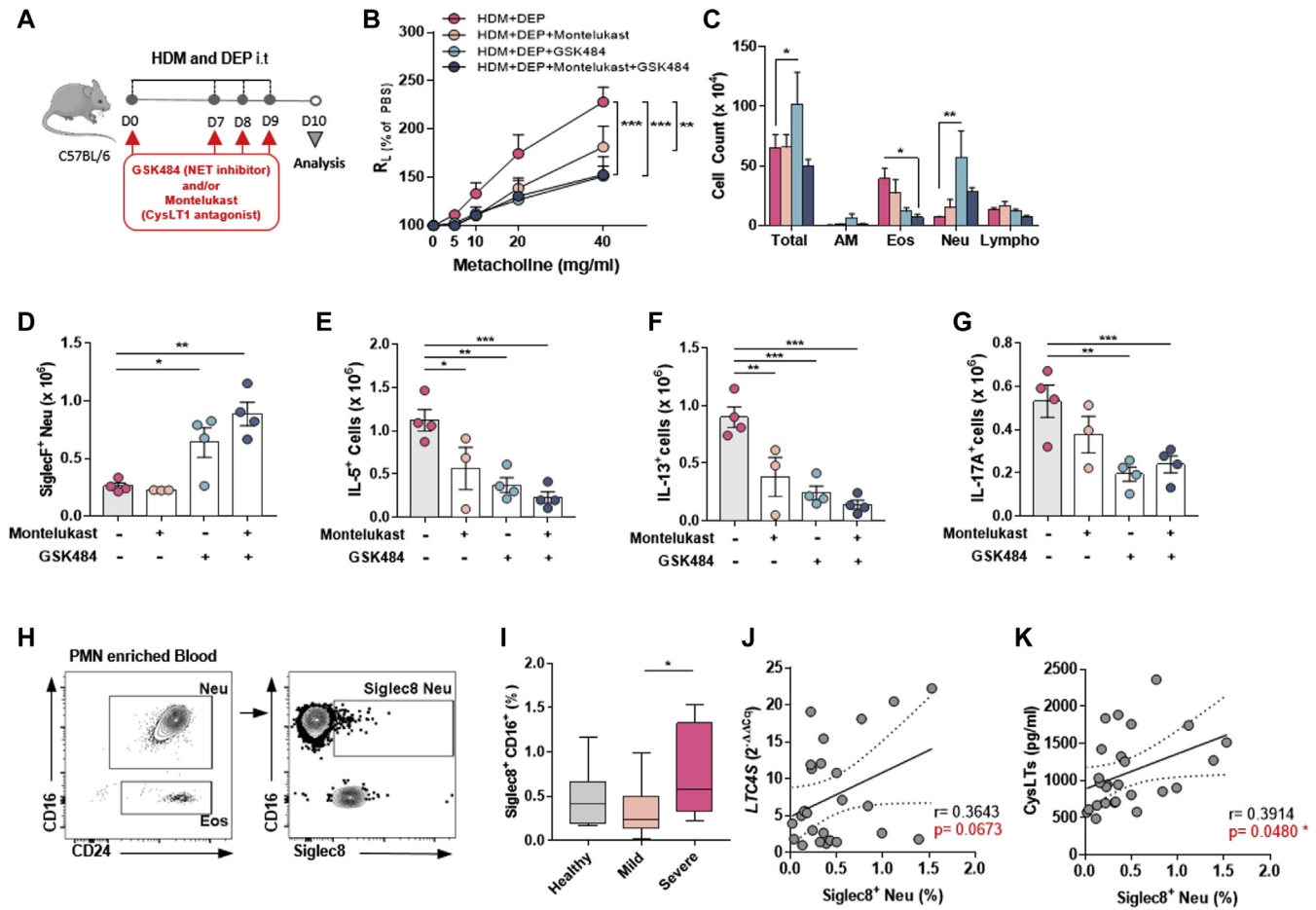


**FIG 7.** The therapeutic effect of NET and CysLT on the DEP-mediated exacerbation of allergic asthma. **A**, Schematic diagram of montelukast and GSK484 treatment. **B, C**, AHR (**B**) and differential BAL fluid immune cell counts (**C**) of HDM + DEP-induced asthma group and montelukast and/or GSK484-treated group. **D**, Quantification of lung SiglecF<sup>+</sup> neutrophils numbers in the groups described in (A). **E–G**, IL-5– (**E**), IL-13– (**F**), and IL-17A– (**G**) positive cells in the groups described in (A) (**B**,  $n = 6$ –8 per group; **C–G**,  $n = 3$ –4 per group). **H**, Neutrophils isolated from the peripheral blood of patients with asthma. **I**, Frequency of blood Siglec8<sup>+</sup> neutrophils in healthy control ( $n = 7$ ), asthma ( $n = 18$ ), and ACO ( $n = 8$ ) patients. **J, K**, Correlation analyses between the Siglec8<sup>+</sup> neutrophils and LTC4S expression (**J**) or plasma CysLT concentrations (**K**) from healthy control and patients with asthma and ACO ( $n = 26$ ). Values are represented as means  $\pm$  SEMs. \* $P < .05$ , \*\* $P < .01$ , \*\*\* $P < .001$ . Dashed lines in (**J**) and (**K**) represent the 5th and 95th percentiles of the distribution of correlation values.

convergent paralog of murine SiglecF,<sup>39</sup> we enumerated the Siglec8<sup>+</sup> neutrophils in patients with asthma ( $n = 18$ ) or ACO ( $n = 8$ ) and in healthy controls ( $n = 7$ ). ACO was reported to be more susceptible to frequent and severe exacerbation,<sup>40–42</sup> although classifying people with asthma as having ACO is still controversial.<sup>43</sup> We found Siglec8<sup>+</sup> neutrophils in the induced sputum of the patients (see Fig E7, A and B, in this article's Online Repository at [www.jacionline.org](http://www.jacionline.org)). Although Siglec8<sup>+</sup> neutrophils in the peripheral blood were few (Fig 7, H), patients with ACO had higher frequencies of circulating Siglec8<sup>+</sup> neutrophils (Fig 7, I). As with murine SiglecF<sup>+</sup> neutrophils, LTC4S and CysLT correlated positively with the frequencies of Siglec8<sup>+</sup> neutrophils in the peripheral blood ( $r = 0.3643$ ,  $P = .07$  and  $r = 0.3917$ ,  $P = .048$ , respectively) (Fig 7, J and K) and significantly elevated in ACO patients (Fig E7, C and D). However, an analysis of NET-associated features (dsDNA) showed no correlation with Siglec8<sup>+</sup> neutrophil in the blood (Fig E7, E and F). These

results suggest that neutrophils similar to SiglecF<sup>+</sup> neutrophils are also present in the asthmatic condition, and they may contribute to the development of asthma.

## DISCUSSION

In the present study, we showed that SiglecF<sup>+</sup> neutrophils may play a hitherto unrecognized role in airway inflammation caused by air-pollutant exposure combined with asthma. We found that SiglecF<sup>+</sup> neutrophils are phenotypically, morphologically, and transcriptionally distinct from conventional neutrophils and eosinophils. These differences mean that these cells produce high levels of ROS, NETs, and CysLTs, and trigger both type 2 and type 3 inflammatory responses. We also confirmed that ACO is associated with similar cells: compared to healthy controls and patients with asthma, patients with ACO had greater numbers of circulating Siglec8<sup>+</sup> neutrophils that resembled murine SiglecF<sup>+</sup> neutrophils.

While we were conducting the present study, Engblom et al<sup>44</sup> reported that SiglecF<sup>+</sup> neutrophils infiltrate lung adenocarcinomas, and Matsui et al<sup>45</sup> showed that SiglecF<sup>+</sup> neutrophils are increased in allergic rhinitis. The fact that this novel immune cell type was discovered in different disease models not only reinforces the findings of all studies but also suggests that the function of SiglecF<sup>+</sup> neutrophils in disease deserve further attention. SiglecF is a representative marker of eosinophils, which generally play a key role in asthma.<sup>46</sup> Therefore, it is important to emphasize that the SiglecF<sup>+</sup> neutrophils we detected are distinct from eosinophils. Previously, Zilionis et al<sup>47</sup> and Pfirsichke et al<sup>48</sup> used transcriptome mapping and immune profiling to show that SiglecF<sup>+</sup>Ly6G<sup>+</sup> cells are bona fide neutrophils. However, they did not determine how closely related SiglecF<sup>+</sup>Ly6G<sup>+</sup> granulocytes are to eosinophils. In the current study, we used eosinophil-deficient  $\Delta$ dflGATA mice to show clearly that SiglecF<sup>+</sup>Ly6G<sup>+</sup> granulocytes are not derived from eosinophils. When these mice were exposed to DEP, their lungs still generated SiglecF<sup>+</sup>Ly6G<sup>+</sup> granulocytes and higher levels of the lipid mediators produced by these cells, namely CysLTs.

In the present study, we further showed that DEP exposure induces SiglecF<sup>+</sup> neutrophils and that they may exacerbate asthma by producing NETs. Specifically, we showed that when asthmatic mice were treated with an inhibitor of NET formation (GSK484), both AHR and the production of inflammatory cytokines in the lungs dropped significantly. This observation is supported by several studies reporting that NET-prone neutrophils are specifically recruited during asthma exacerbation.<sup>21,49,50</sup> Moreover, the major causes of asthma exacerbation, bacterial infection<sup>51</sup> and cigarette smoke,<sup>52</sup> are associated with NET formation.

Several of our experiments also suggest that SiglecF<sup>+</sup> neutrophils may worsen asthma by producing high levels of CysLTs in the lungs, which in turn promote the local production of type 2 cytokines. Previous study has shown that neutrophil-attached platelets contribute to CysLT production.<sup>53</sup> Although SiglecF<sup>+</sup> neutrophils expressing the platelet markers, such as CD41 and CD42d, were not increased by DEP exposure (data not shown), the possibility that the CysLT increase was due to interaction with platelets cannot be completely excluded. Nevertheless, we showed that SiglecF<sup>+</sup> neutrophils from DEP-exposed lungs produced significant amounts of CysLTs on phorbol 12-myristate 13-acetate/ionomycin stimulation. Moreover, when these cells were co-cultured with T<sub>H</sub>2 cells, the T cells produced higher levels of IL-5 and IL-13. Second, while adoptive transfer of SiglecF<sup>+</sup> neutrophils worsened asthma, this was not observed when these cells had been pretreated with a CysLT production-disrupting agent. This asthmogenic effect of CysLTs is supported by several studies showing that CysLTs generated by eosinophils, mast cells, and basophils can worsen the symptoms of asthma and that this effect is mediated by increasing type 2 inflammation, vascular permeability, and bronchial smooth muscle contraction.<sup>54-56</sup> Notably, Castellani et al<sup>57</sup> have shown that CysLTs may induce neutrophilia in asthma by causing T<sub>H</sub>2 cells to produce cytokines such as granulocyte-macrophage colony-stimulating factor, which prime neutrophils to release NET in the airways, and IL-8, which attracts and activates neutrophils.<sup>58</sup> Hence, we believe that cross talk between T<sub>H</sub>2 cells (and ILC2s) and SiglecF<sup>+</sup> neutrophils may enhance the inflammatory response synergistically during asthma progression.

It remains unclear how DEP exposure induces SiglecF<sup>+</sup> neutrophils in the lung. Engblom et al<sup>44</sup> suggested that SiglecF<sup>+</sup> neutrophils in lung adenocarcinoma were derived from osteoblasts in the BM, which suggests these cells were recruited from other tissues. However, in our case, it is possible that SiglecF<sup>+</sup> neutrophils in the lung differentiated from lung resident neutrophils: we showed that the BAL fluid of DEP-treated mice (namely, the lung microenvironment) induced BM-derived neutrophils to express SiglecF. DEP by itself did not have this effect, regardless of dose or time. The nature of the DEP-induced triggering microenvironment is not entirely clear, but we observed that SiglecF<sup>+</sup> neutrophils express higher levels of the P2X1 receptor, which recognizes extracellular ATP, a damage-associated molecular pattern (DAMP) signaling molecule. DEP also upregulated extracellular ATP levels in the lung. Moreover, intratracheal treatment of ATP led to the development of SiglecF<sup>+</sup> neutrophils. It is well known that sites of tissue damage can contain DAMPs along with cytokines, pathogen-associated molecular patterns, and various environmental factors.<sup>59,60</sup> It remains unclear how DAMP signaling induces SiglecF expression, but multiple studies suggest it may be mediated by the ATP-dependent nucleosome-remodeling complexes that are involved in the dynamic regulation of chromatin.<sup>61</sup> Thus, to elucidate the mechanisms by which SiglecF<sup>+</sup> neutrophils develop and the heterogeneity of neutrophils, further analysis of the epigenetic changes that occur in response to environmental stimuli will be needed.

In conclusion, we discovered that SiglecF<sup>+</sup> neutrophils, which have unique features, play a novel role in asthma exacerbation. We speculate that these cells are induced by environmental risk factors such as air pollution that promote the release of DAMP signals. These findings expand our understanding of granulocytes, which are generally thought to be mere mediators of inflammation. Our results show that in fact, SiglecF<sup>+</sup> neutrophils may promote both type 2 and type 3 immune responses by releasing NETs and producing CysLT. The translational experiments also suggest that Siglec8<sup>+</sup> neutrophils may contribute to the pathogenesis of ACO in humans. Although most of the latter experiments were performed with peripheral blood rather than sputum and with a small number of samples (a result of limitations in the human samples) and although correlations were weak, we observed that Siglec8<sup>+</sup> neutrophil numbers rose with worsening asthma. Thus, the identification of these neutrophils may provide an opportunity for devising alternative therapeutic strategies for asthma and suggest new ways to interrogate the neutrophil response to environmental stimuli.

We thank Dale T. Umetsu (Stanford University) for valuable comments.

### Key messages

- Air pollutants induce SiglecF expression on neutrophil via DAMP signals such as extracellular ATP.
- SiglecF<sup>+</sup> neutrophils aggravate both type 2 and type 3 immune-related asthma by producing CysLTs and NETs.
- The human equivalent of murine SiglecF<sup>+</sup> neutrophils, Siglec8<sup>+</sup> neutrophils, was significantly more frequent in the circulation of patients with ACO than in patients with asthma or in healthy controls.

## REFERENCES

- Lundback B, Backman H, Lotvall J, Ronmark E. Is asthma prevalence still increasing? *Expert Rev Respir Med* 2016;10:39-51.
- Holgate ST, Wenzel S, Postma DS, Weiss ST, Renz H, Sly PD. Asthma. *Nat Rev Dis Primers* 2015;1:15025.
- Bateman ED, Hurd SS, Barnes PJ, Bousquet J, Drazen JM, FitzGerald JM, et al. Global strategy for asthma management and prevention: GINA executive summary. *Eur Respir J* 2008;31:143-78.
- D'Amato G, Liccardi G, D'Amato M, Holgate S. Environmental risk factors and allergic bronchial asthma. *Clin Exp Allergy* 2005;35:1113-24.
- Kim J, Natarajan S, Vaickus LJ, Bouchard JC, Beal D, Cruikshank WW, et al. Diesel exhaust particulates exacerbate asthma-like inflammation by increasing CXC chemokines. *Am J Pathol* 2011;179:2730-9.
- Brandt EB, Myers JM, Ryan PH, Hershey GK. Air pollution and allergic diseases. *Curr Opin Pediatr* 2015;27:724-35.
- Murrison LB, Brandt EB, Myers JB, Hershey GKK. Environmental exposures and mechanisms in allergy and asthma development. *J Clin Invest* 2019;129:1504-15.
- Wenzel SE. Asthma phenotypes: the evolution from clinical to molecular approaches. *Nat Med* 2012;18:716-25.
- Kuruvilla ME, Lee FE, Lee GB. Understanding asthma phenotypes, endotypes, and mechanisms of disease. *Clin Rev Allergy Immunol* 2019;56:219-33.
- Lambrecht BN, Hammad H. Dendritic cell and epithelial cell interactions at the origin of murine asthma. *Ann Am Thorac Soc* 2014;11(suppl 5):S236-43.
- Bousquet J, Chanez P, Lacoste JY, Barneon G, Ghavarian N, Enander I, et al. Eosinophilic inflammation in asthma. *N Engl J Med* 1990;323:1033-9.
- Lambrecht BN, Persson EK, Hammad H. Myeloid cells in asthma. *Microbiol Spectr* 2017;5(1).
- Galli SJ, Tsai M. IgE and mast cells in allergic disease. *Nat Med* 2012;18:693-704.
- Nadif R, Siroux V, Boudier A, le Moual N, Just J, Gormand F, et al. Blood granulocyte patterns as predictors of asthma phenotypes in adults from the EGEA study. *Eur Respir J* 2016;48:1040-51.
- Hastie AT, Moore WC, Meyers DA, Vestal PL, Li H, Peters SP, et al. Analyses of asthma severity phenotypes and inflammatory proteins in subjects stratified by sputum granulocytes. *J Allergy Clin Immunol* 2010;125:1028-36.e13.
- McKinley L, Alcorn JF, Peterson A, Dupont RB, Kapadia S, Logar A, et al. T<sub>H</sub>17 cells mediate steroid-resistant airway inflammation and airway hyperresponsiveness in mice. *J Immunol* 2008;181:4089-97.
- Goleva E, Hauk PJ, Hall CF, Liu AH, Riches DW, Martin RJ, et al. Corticosteroid-resistant asthma is associated with classical antimicrobial activation of airway macrophages. *J Allergy Clin Immunol* 2008;122:550-9.e3.
- Kim HY, Lee HJ, Chang YJ, Pichavant M, Shore SA, Fitzgerald KA, et al. Interleukin-17-producing innate lymphoid cells and the NLRP3 inflammasome facilitate obesity-associated airway hyperreactivity. *Nat Med* 2014;20:54-61.
- Kudo M, Melton AC, Chen C, Engler MB, Huang KE, Ren X, et al. IL-17A produced by alphabeta T cells drives airway hyper-responsiveness in mice and enhances mouse and human airway smooth muscle contraction. *Nat Med* 2012;18:547-54.
- Radermecker C, Louis R, Bureau F, Marichal T. Role of neutrophils in allergic asthma. *Curr Opin Immunol* 2018;54:28-34.
- Toussaint M, Jackson DJ, Swieboda D, Guedan A, Tsourouktoglou TD, Ching YM, et al. Host DNA released by NETosis promotes rhinovirus-induced type-2 allergic asthma exacerbation. *Nat Med* 2017;23:681-91.
- Papayannopoulos V. Neutrophil extracellular traps in immunity and disease. *Nat Rev Immunol* 2018;18:134-47.
- Dunnill MS. Quantitative methods in the study of pulmonary pathology. *Thorax* 1962;17:320-8.
- Kotecha N, Krutzik PO, Irish JM. Web-based analysis and publication of flow cytometry experiments. *Curr Protoc Cytom* 2010;Chapter 10:Unit10 7.
- Brinkmann V, Laube B, Abu Abed U, Goosmann C, Zychlinsky A. Neutrophil extracellular traps: how to generate and visualize them. *J Vis Exp* 2010;(36):1724.
- Yu C, Cantor AB, Yang H, Browne C, Wells RA, Fujiwara Y, et al. Targeted deletion of a high-affinity GATA-binding site in the GATA-1 promoter leads to selective loss of the eosinophil lineage in vivo. *J Exp Med* 2002;195:1387-95.
- Bindea G, Mlecnik B, Hackl H, Charoentong P, Tosolini M, Kirilovsky A, et al. ClueGO: a Cytoscape plug-in to decipher functionally grouped gene ontology and pathway annotation networks. *Bioinformatics* 2009;25:1091-3.
- Shannon P, Markiel A, Ozier O, Baliga NS, Wang JT, Ramage D, et al. Cytoscape: a software environment for integrated models of biomolecular interaction networks. *Genome Res* 2003;13:2498-504.
- Kassack MU, Braun K, Ganso M, Ullmann H, Nickel P, Boing B, et al. Structure-activity relationships of analogues of NF449 confirm NF449 as the most potent and selective known P2X1 receptor antagonist. *Eur J Med Chem* 2004;39:345-57.
- Idzko M, Ferrari D, Eltzschig HK. Nucleotide signalling during inflammation. *Nature* 2014;509(7500):310-7.
- Lood C, Blanco LP, Purmalek MM, Carmona-Rivera C, De Ravin SS, Smith CK, et al. Neutrophil extracellular traps enriched in oxidized mitochondrial DNA are interferogenic and contribute to lupus-like disease. *Nat Med* 2016;22:146-53.
- Metzler KD, Goosmann C, Lubojemska A, Zychlinsky A, Papayannopoulos V. A myeloperoxidase-containing complex regulates neutrophil elastase release and actin dynamics during NETosis. *Cell Rep* 2014;8:883-96.
- Dicker AJ, Crichton ML, Pumphrey EG, Cassidy AJ, Suarez-Cuartin G, Sibila O, et al. Neutrophil extracellular traps are associated with disease severity and microbiota diversity in patients with chronic obstructive pulmonary disease. *J Allergy Clin Immunol* 2018;141:117-27.
- Grabcanyic-Musija F, Obermayer A, Stoiber W, Krautgartner WD, Steinbacher P, Winterberg N, et al. Neutrophil extracellular trap (NET) formation characterises stable and exacerbated COPD and correlates with airflow limitation. *Respir Res* 2015;16:59.
- Lewis HD, Liddle J, Coote JE, Atkinson SJ, Barker MD, Bax BD, et al. Inhibition of PAD4 activity is sufficient to disrupt mouse and human NET formation. *Nat Chem Biol* 2015;11:189-91.
- Funk CD. Prostaglandins and leukotrienes: advances in eicosanoid biology. *Science* 2001;294(5548):1871-5.
- Gillard J, Ford-Hutchinson AW, Chan C, Charleson S, Denis D, Foster A, et al. L-663,536 (MK-886)(3-[1-(4-chlorobenzyl)-3-t-butyl-thio-5-isopropylindol-2-yl]-2,2-dimethylpropanoic acid), a novel, orally active leukotriene biosynthesis inhibitor. *Can J Physiol Pharmacol* 1989;67:456-64.
- Leff JA, Busse WW, Pearlman D, Bronsky EA, Kemp J, Hendeles L, et al. Montelukast, a leukotriene-receptor antagonist, for the treatment of mild asthma and exercise-induced bronchoconstriction. *N Engl J Med* 1998;339:147-52.
- Tateno H, Crocker PR, Paulson JC. Mouse Siglec-F and human Siglec-8 are functionally convergent paralogs that are selectively expressed on eosinophils and recognize 6'-sulfo-sialyl Lewis X as a preferred glycan ligand. *Glycobiology* 2005;15:1125-35.
- de Marco R, Pesce G, Marcon A, Accordini S, Antonicelli L, Bugiani M, et al. The coexistence of asthma and chronic obstructive pulmonary disease (COPD): prevalence and risk factors in young, middle-aged and elderly people from the general population. *PLoS One* 2013;8:e62985.
- Hardin M, Silverman EK, Barr RG, Hansel NN, Schroeder JD, Make BJ, et al. The clinical features of the overlap between COPD and asthma. *Respir Res* 2011;12:127.
- Kauppi P, Kupiainen H, Lindqvist A, Tammilehto L, Kilpelainen M, Kinnula VL, et al. Overlap syndrome of asthma and COPD predicts low quality of life. *J Asthma* 2011;48:279-85.
- Xia Y, Cao Y, Xia L, Li W, Shen H. Severe asthma and asthma-COPD overlap: a double agent or identical twins? *J Thorac Dis* 2017;9:4798-805.
- Engblom C, Pfirsichke C, Zilionis R, Da Silva Martins J, Bos SA, Courties G, et al. Osteoblasts remotely supply lung tumors with cancer-promoting SiglecF<sup>high</sup> neutrophils. *Science* 2017;358(6367):eaal5081.
- Matsui M, Nagakubo D, Satooka H, Hirata T. A novel Siglec-F<sup>+</sup> neutrophil subset in the mouse nasal mucosa exhibits an activated phenotype and is increased in an allergic rhinitis model. *Biochem Biophys Res Commun* 2020;526:599-606.
- Kim HY, DeKruyff RH, Umetsu DT. The many paths to asthma: phenotype shaped by innate and adaptive immunity. *Nat Immunol* 2010;11:577-84.
- Zilionis R, Engblom C, Pfirsichke C, Savova V, Zemmour D, Saatcioglu HD, et al. Single-cell transcriptomics of human and mouse lung cancers reveals conserved myeloid populations across individuals and species. *Immunity* 2019;50:1317-34.e10.
- Pfirsichke C, Engblom C, Gungabeesoon J, Lin Y, Rickelt S, Zilionis R, et al. Tumor-promoting Ly-6G<sup>+</sup> SiglecF<sup>high</sup> cells are mature and long-lived neutrophils. *Cell Rep* 2020;32:108164.
- Krishnamoorthy N, Douda DN, Bruggemann TR, Ricklef I, Duvall MG, Abdulnour RE, et al. Neutrophil cytoplasts induce T<sub>H</sub>17 differentiation and skew inflammation toward neutrophilia in severe asthma. *Sci Immunol* 2018;3(26):eaao4747.
- Pham DL, Ban GY, Kim SH, Shin YS, Ye YM, Chwae YJ, et al. Neutrophil autophagy and extracellular DNA traps contribute to airway inflammation in severe asthma. *Clin Exp Allergy* 2017;47:57-70.
- Iikura M, Hojo M, Koketsu R, Watanabe S, Sato A, Chino H, et al. The importance of bacterial and viral infections associated with adult asthma exacerbations in clinical practice. *PLoS One* 2015;10:e0123584.
- Chaudhuri R, Livingston E, McMahon AD, Thomson L, Borland W, Thomson NC. Cigarette smoking impairs the therapeutic response to oral corticosteroids in chronic asthma. *Am J Respir Crit Care Med* 2003;168:1308-11.

53. Laidlaw TM, Kidder MS, Bhattacharyya N, Xing W, Shen S, Milne GL, et al. Cysteinyl leukotriene overproduction in aspirin-exacerbated respiratory disease is driven by platelet-adherent leukocytes. *Blood* 2012;119:3790-8.
54. Accomazzo MR, Rovati GE, Vigano T, Hernandez A, Bonazzi A, Bolla M, et al. Leukotriene D4-induced activation of smooth-muscle cells from human bronchi is partly  $\text{Ca}^{2+}$ -independent. *Am J Respir Crit Care Med* 2001;163:266-72.
55. Peters-Golden M, Henderson WR Jr. Leukotrienes. *N Engl J Med* 2007;357:1841-54.
56. Parmentier CN, Fuerst E, McDonald J, Bowen H, Lee TH, Pease JE, et al. Human  $\text{T}_{\text{H}}2$  cells respond to cysteinyl leukotrienes through selective expression of cysteinyl leukotriene receptor 1. *J Allergy Clin Immunol* 2012;129:1136-42.
57. Castellani S, D'Oria S, Diana A, Polizzi AM, Di Gioia S, Mariggio MA, et al. G-CSF and GM-CSF modify neutrophil functions at concentrations found in cystic fibrosis. *Sci Rep* 2019;9:12937.
58. Degroote RL, Weigand M, Hauck SM, Deeg CA. IL8 and PMATrigger the regulation of different biological processes in granulocyte activation. *Front Immunol* 2019;10:3064.
59. Zindel J, Kubes P. DAMPs, PAMPs, and LAMPs in immunity and sterile inflammation. *Annu Rev Pathol* 2020;15:493-518.
60. Gong T, Liu L, Jiang W, Zhou R. DAMP-sensing receptors in sterile inflammation and inflammatory diseases. *Nat Rev Immunol* 2020;20:95-112.
61. Clapier CR, Iwasa J, Cairns BR, Peterson CL. Mechanisms of action and regulation of ATP-dependent chromatin-remodelling complexes. *Nat Rev Mol Cell Biol* 2017;18:407-22.

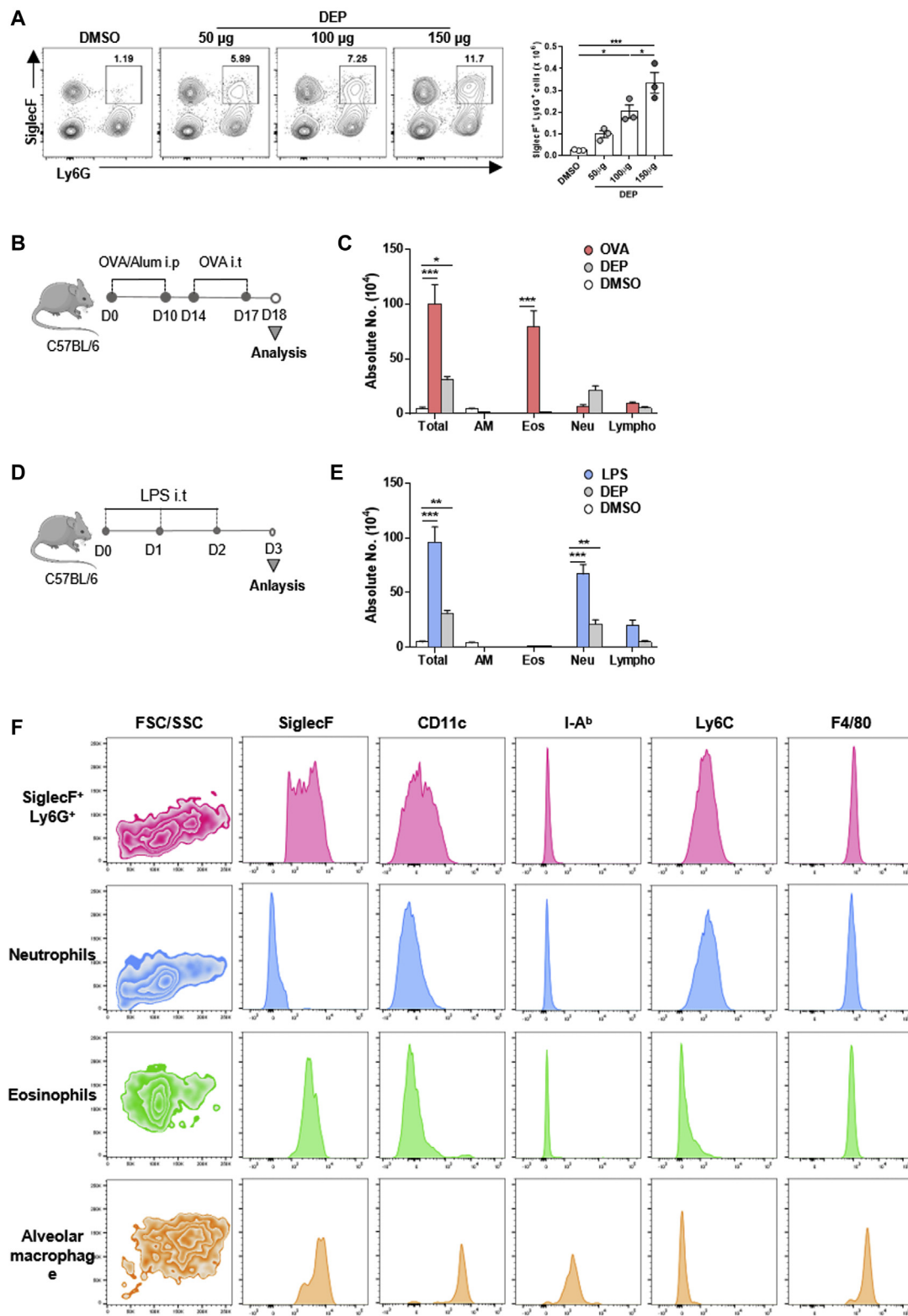


**FIG E1.** SiglecF<sup>+</sup>Ly6G<sup>+</sup> granulocytes do not exist in the lungs from OVA-induced asthma and LPS-induced acute lung injury. **A**, Representative dot plot (A) of SiglecF<sup>+</sup>Ly6G<sup>+</sup> granulocytes in vehicle, 50 µg, 100 µg, and 150 µg of DEP-exposed lung. **B**, Schematic diagram of OVA-induced asthma. **C**, Differential counting of BAL fluid immune cells from DMSO-, DEP-, and OVA-treated lungs. **D**, Schematic diagram of LPS-induced acute lung injury. **E**, Differential counting of BAL fluid immune cells from DMSO-, DEP-, and LPS-treated lungs. **F**, Alveolar macrophages, eosinophils, neutrophils, and SiglecF<sup>+</sup>Ly6G<sup>+</sup> granulocytes from DEP-exposed lungs were examined for the expression of indicated surface markers, granularity, and size. Data are pooled from 2 independent experiments (B-E) or are representative of 3 independent experiments (A, F) with values represented as means ± SEMs. \* $P < .05$ , \*\* $P < .01$ , \*\*\* $P < .001$ , 1-way ANOVA (A) or 2-way ANOVA (D, F) with Tukey post hoc test.

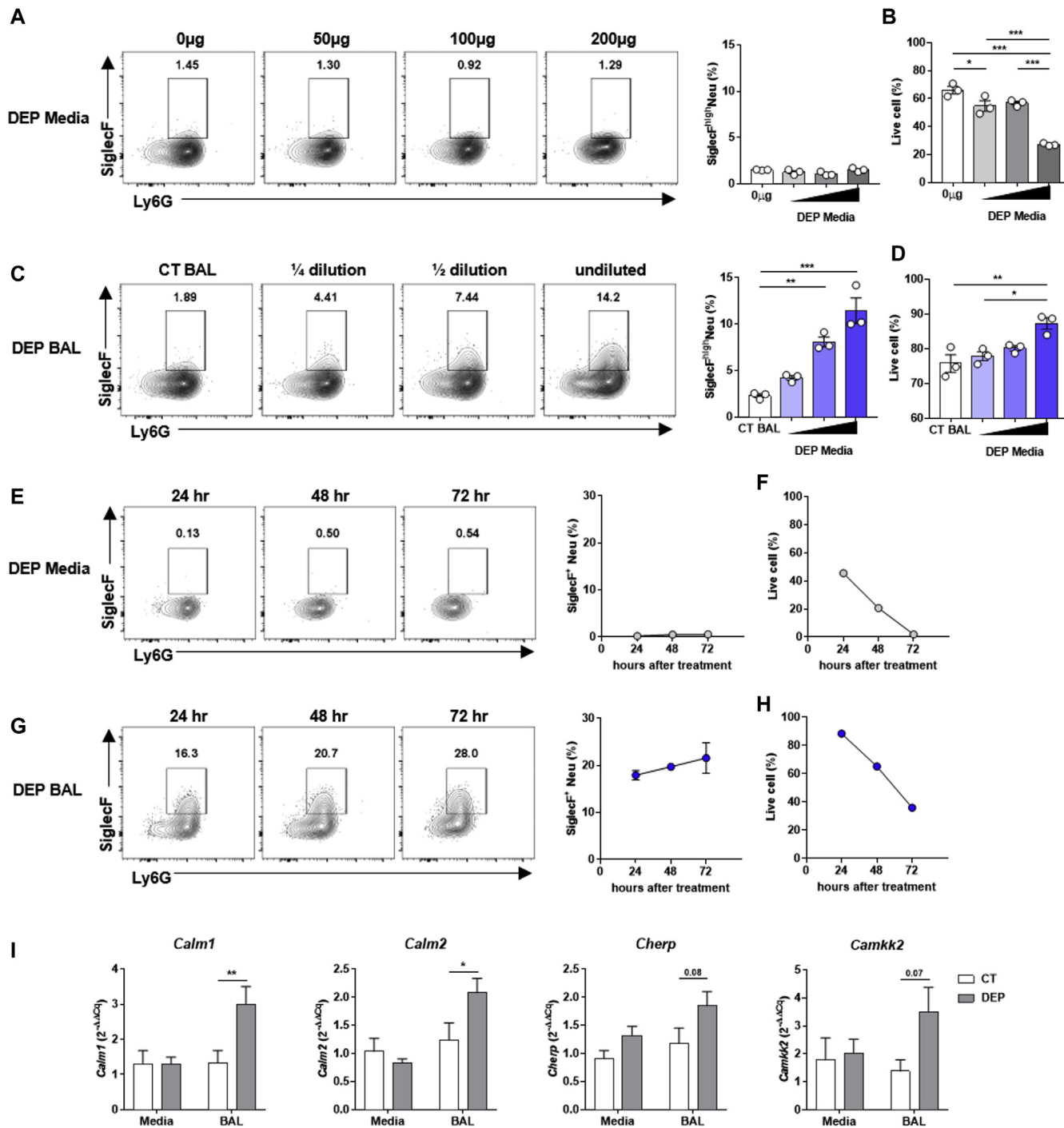


**FIG E2.** SigurecF expression on BM neutrophils is induced by DEP BAL, but not DEP media, in a dose- and time-dependent manner. **A, B**, SigurecF expression (A) and viability (B) of BM neutrophils cultured with DEP (0, 50, 100, and 200 µg/mL) dissolved media for 48 hours. **C, D**, SigurecF expression (C) and viability (D) of BM neutrophils cultured with BAL from DEP-treated mice for 48 hours. **E, F**, SigurecF expression (E) and viability (F) of BM neutrophils cultured with DEP (100 µg/mL) dissolved media. **G, H**, SigurecF expression (G) and viability (H) of BM neutrophils cultured with BAL from DEP-treated mice. **I**, Relative expression of *Calm1*, *Calm2*, *Cherp*, and *Camkk2* of BM neutrophils cultured with DEP media or BAL for 48 hours. Data are pooled from 2 independent experiments (I) or are representative of 3 independent experiments (A-H) with values represented as means ± SEMs. \*P < .05, \*\*P < .01, \*\*\*P < .001, 1-way ANOVA (A, B, E, F) or 2-way ANOVA (I) with Tukey post hoc test.

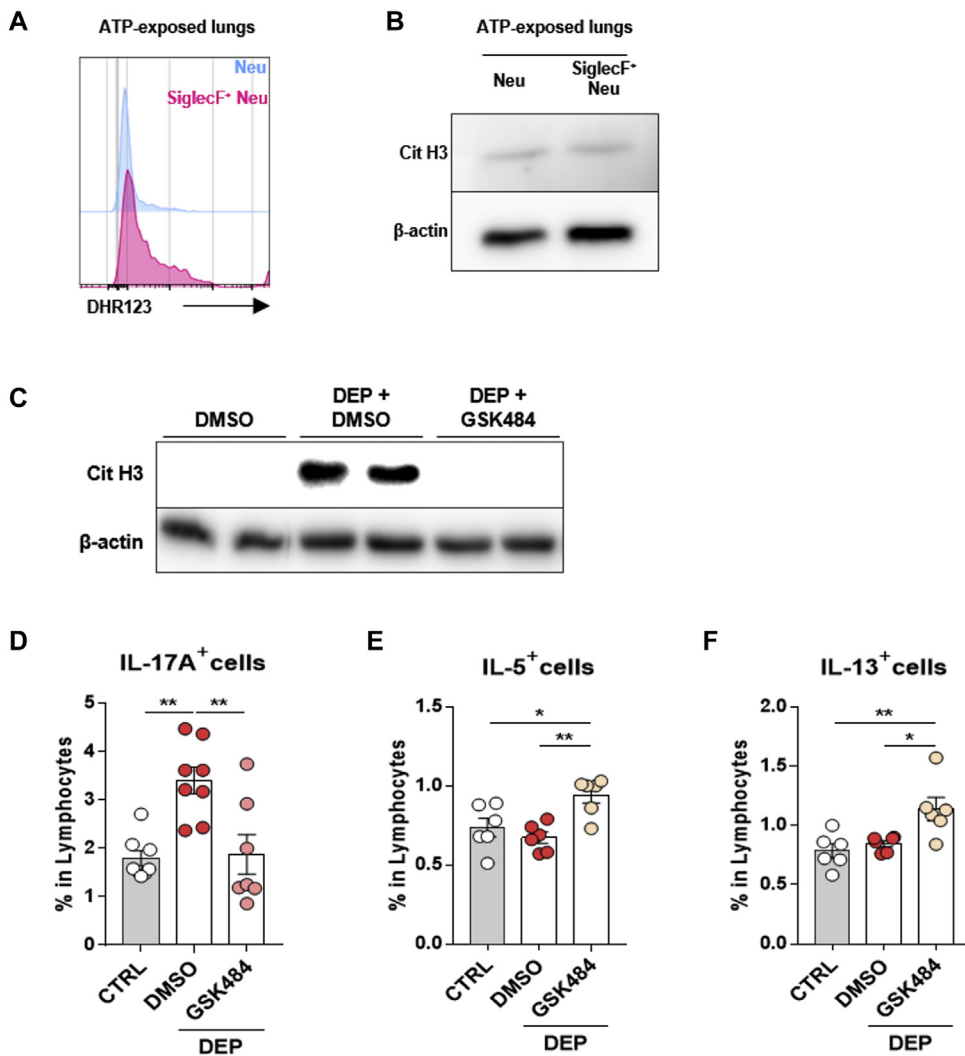


**FIG E3.** The NET inhibitor GSK484 alleviated lung histone citrullination and IL-17 production. **A**, Histogram of dihydrorhodamine (DHR) 123 expressions of conventional and SiglecF<sup>+</sup> neutrophils of ATP-exposed lungs. **B**, Western blot analysis of CitH3 of conventional and SiglecF<sup>+</sup> neutrophils of ATP-exposed lungs. **C**, Western blot analysis of CitH3 from a vehicle, DEP + DMSO-, and DEP + GSK484-treated lung lysates. **D-F**, Representative bar graphs of the frequencies of IL-17A (**D**), IL-5 (**E**), and IL-13 (**F**) cytokine production for each group (**D**, n = 7-8 per group; **E, F**, n = 6 per group). Data are pooled from 3 independent experiments (**D-F**) or are representative of 3 independent experiments (**A-C**) with values represented as means  $\pm$  SEMs. \*P < .05, \*\*P < .01, \*\*\*P < .001, 1-way ANOVA (**D-F**) with Tukey post hoc test.

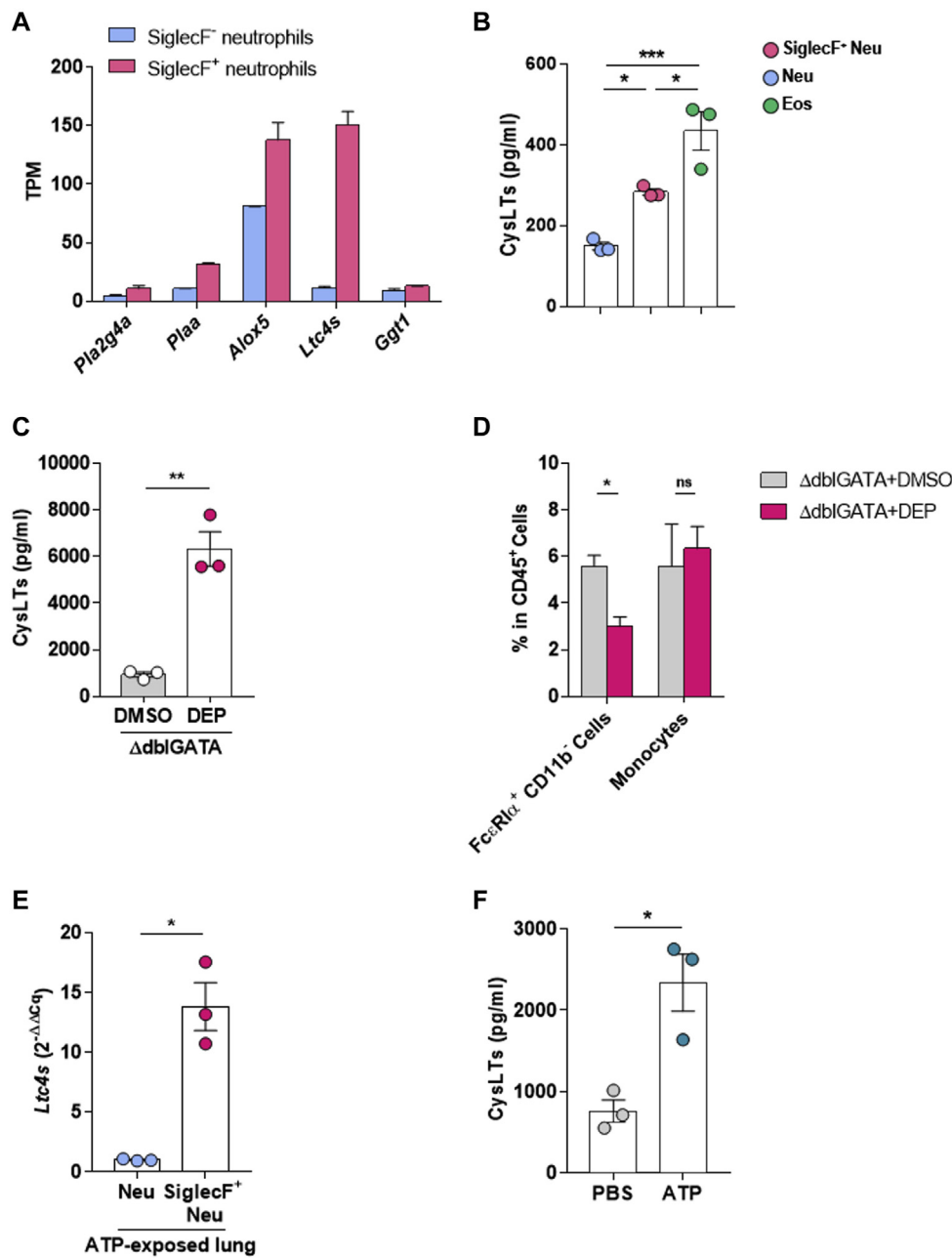


**FIG E4.** Characteristics of SiglecF $^+$  neutrophils. **A**, Transcripts per million (TPM) of CysLT synthesis-associated genes of conventional (SiglecF $^-$ ) and SiglecF $^+$  neutrophils from DEP-exposed mice. **B**, CysLT levels in eosinophils, and conventional and SiglecF $^+$  neutrophils from DEP-exposed lungs. **C**, D, CysLT levels in the BAL fluid (C), and frequencies (D) of  $Fc\epsilon R\alpha^+ CD11b^-$  population and monocytes in wild-type and  $\Delta$ dblGATA mice after DEP exposure (n = 3 per group). **E**, Relative expression of *Ltc4s* of sorted conventional and SiglecF $^+$  neutrophils from ATP-exposed lungs. **F**, CysLT levels in BAL fluids of ATP-exposed mice. Data are representative of 3 independent experiments (B-F) with values represented as means  $\pm$  SEMs \*P < .05, \*\*P < .01, \*\*\*P < .001, unpaired 2-tailed Student *t* test (C, E, F) and 1-way ANOVA (B) or 2-way ANOVA (D) with Tukey post hoc test.

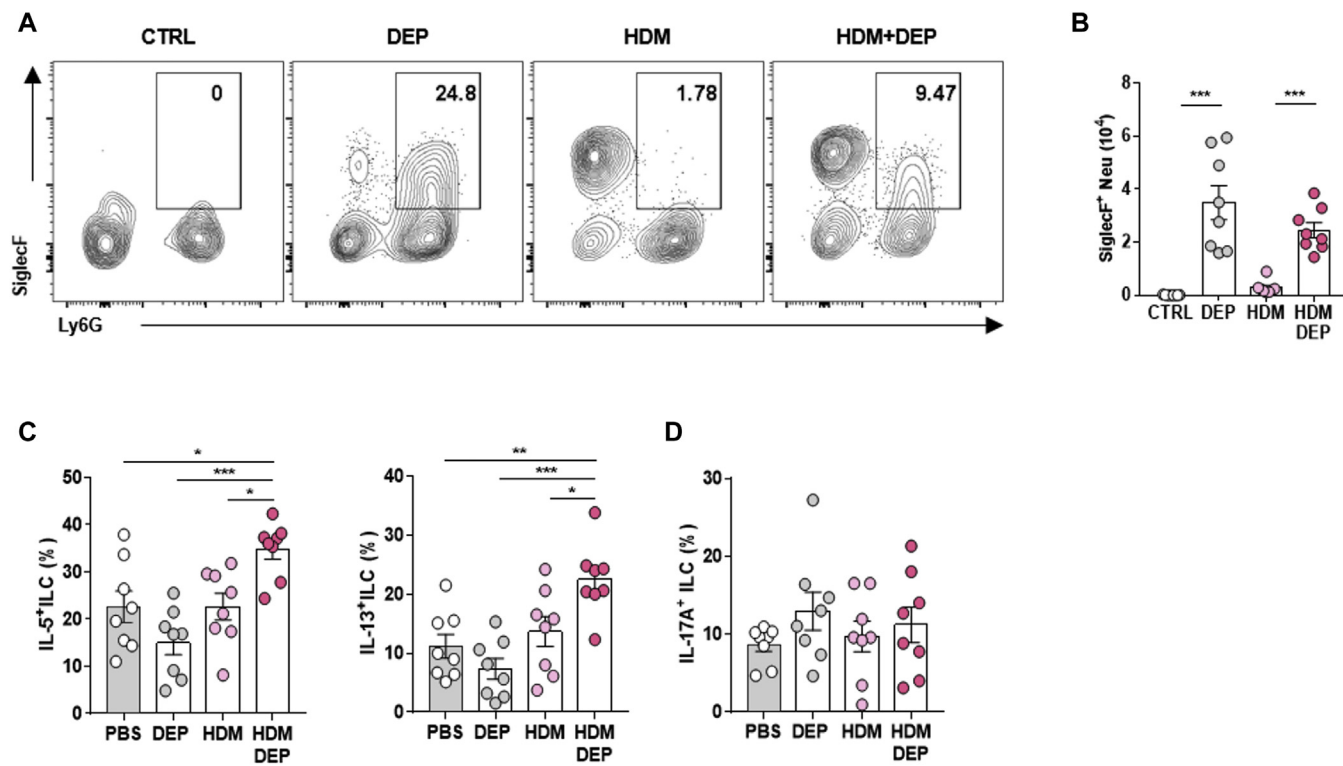


**FIG E5.** SiglecF<sup>+</sup> neutrophils in HDM + DEP-mediated asthma and cytokine productions from ILCs. **A, B,** Representative flow cytometric dot plots of SiglecF<sup>+</sup> neutrophils (A) and quantification of SiglecF<sup>+</sup> neutrophil numbers (B). **C, D,** Frequencies of IL-5<sup>+</sup>, IL-13<sup>+</sup> (C), and IL-17A<sup>+</sup> (D) producing ILCs. Data are pooled from 2 independent experiments (A-D, n = 8 per group) with values represented as means  $\pm$  SEMs. \*P < .05, \*\*P < .01, \*\*\*P < .001, 1-way ANOVA (B-D) with Tukey post hoc test.

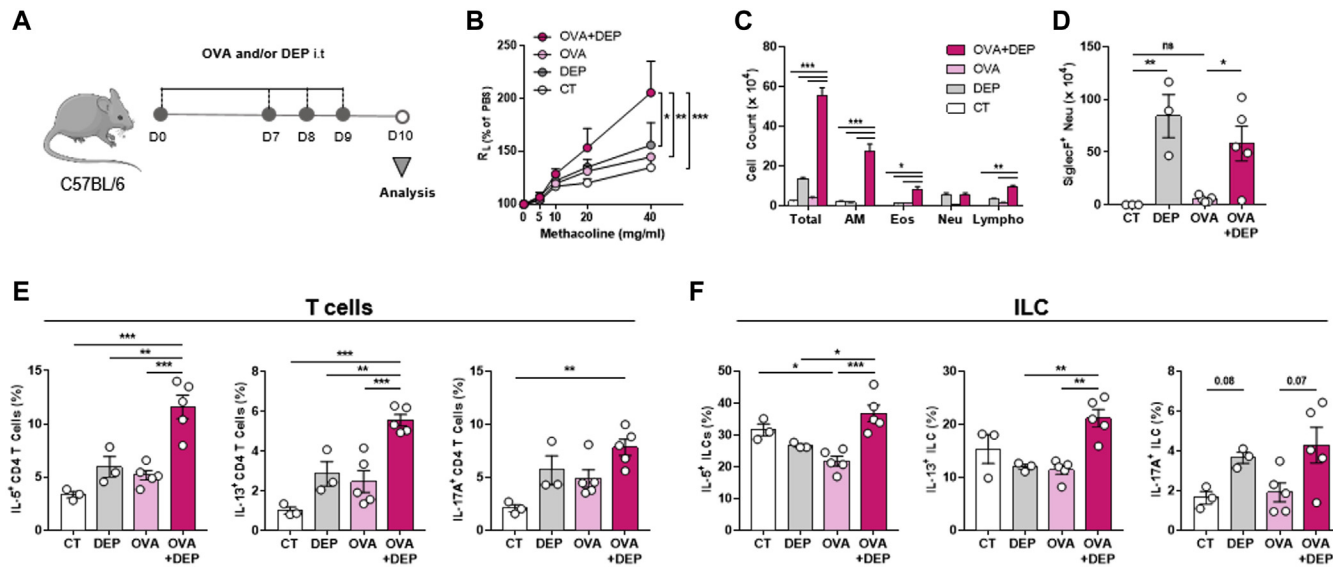


**FIG E6.** Combination treatment of OVA- and DEP-induced asthma model. **A**, Experimental protocol of OVA and DEP treatment. **B**, **C**, AHR (**B**) and differential BAL fluid immune cell counts (**C**) of each group described in (**A**). **D**, Absolute numbers of SiglecF<sup>+</sup> neutrophils of each group. **E**, **F**, Frequencies of IL-5-, IL-13-, and IL-17A-positive CD4 T cells (**E**) and ILCs (**F**). Data are pooled from 3 independent experiments (**B**, **C**) or are representative of 3 independent experiments (**D-F**) with values represented as means  $\pm$  SEMs. \* $P < .05$ , \*\* $P < .01$ , \*\*\* $P < .001$ , 1-way ANOVA (**D-F**) or 2-way ANOVA (**B-C**) with Tukey post hoc test.

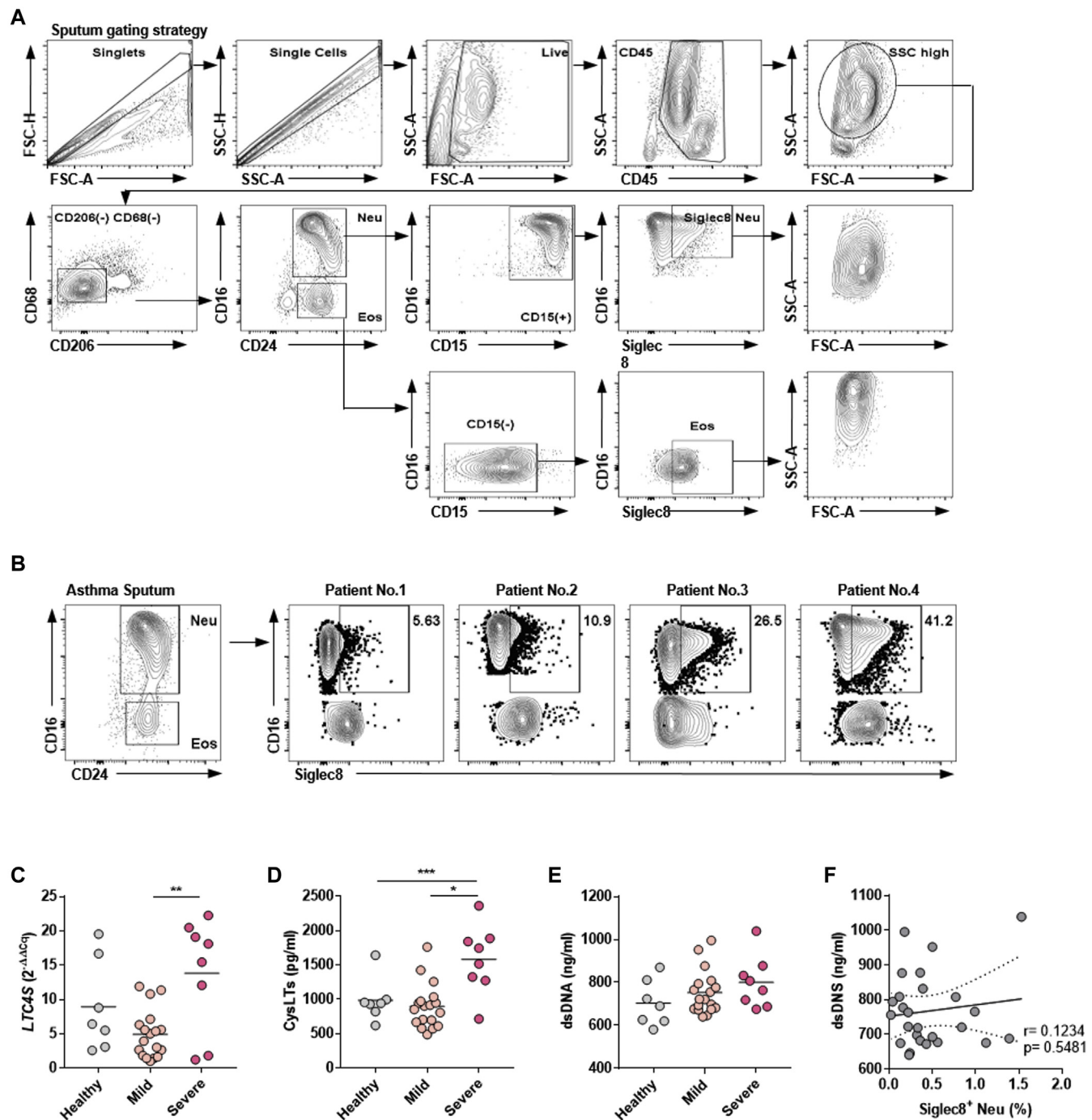


**FIG E7.** Analysis of immune cells in the blood and sputum from healthy control, asthma, and ACO patients. **A**, Gating strategy of eosinophils, neutrophils, and Siglec8<sup>+</sup> neutrophils in the induced sputum. **B**, Representative flow cytometric dot plots of Siglec8<sup>+</sup> neutrophils in the induced sputum. **C, D**, LTC4S mRNA from neutrophils (**C**), and CysLT concentrations in plasma (**D**) from healthy control, asthma, and ACO patients. **E**, Plasma dsDNA levels from healthy control, asthma, and ACO patients. **F**, Correlation analysis between the Siglec8<sup>+</sup> neutrophils and dsDNA concentrations. Values are represented as means  $\pm$  SEMs. \* $P < .05$ , \*\* $P < .01$ , \*\*\* $P < .001$ , 1-way ANOVA (**C-E**) with Tukey post hoc test or Pearson correlation test (**F**). Dashed line in (**F**) represents the 5th and 95th percentiles of the distribution of correlation values.

**TABLE E1.** Comparison of subjects according to asthma severity

Characteristic	Healthy control	Mild asthma	Severe asthma	P value
No. of subjects	7	18	8	
Age (years)	31.00 ± 5.802	55.13 ± 9.858	72 ± 8.502	< .001
FEV <sub>1</sub> (mL)	NA	1684 ± 681.2	1290 ± 428.3	.15
FEV <sub>1</sub> (%)	NA	75.63 ± 24.36	59.13 ± 16.63	.10
FVC (mL)	NA	2268 ± 909.6	2309 ± 587.3	.91
FVC (%)	NA	80.31 ± 21.05	79.38 ± 21.84	.92
FEV <sub>1</sub> /FVC ratio	NA	75.49 ± 11.22	56.63 ± 15.59	.003
Smoking history				
Never	5 (71)	18 (100)	3 (38)	
Ex	2 (29)	0	3 (38)	
Current	0	0	2 (25)	
Steroid treatment	NA	7 (39)	6 (75)	
Peripheral blood testing results				
WBC ( $\times 10^6$ /L)	NA	6059 ± 1878	7775 ± 2256	.12
Eosinophils (%)	NA	4.393 ± 3.753	1.838 ± 0.795	.08
Neutrophils (%)	NA	55.4 ± 10.787	61.81 ± 8.338	.19

Data are expressed as means ± SDs or as no. (%). FEV<sub>1</sub>, Forced expiratory volume in 1 second; FVC, forced vital capacity; NA, not applicable; WBC, white blood cell count.